GOVERNMENT OF BANGLADESH
FLOOD PLAN COORDINATION ORGANIZATION

FAP 24 RIVER SURVEY PROJECT

Remote sensing for morphological assessment
and
radar remote sensing pilot project

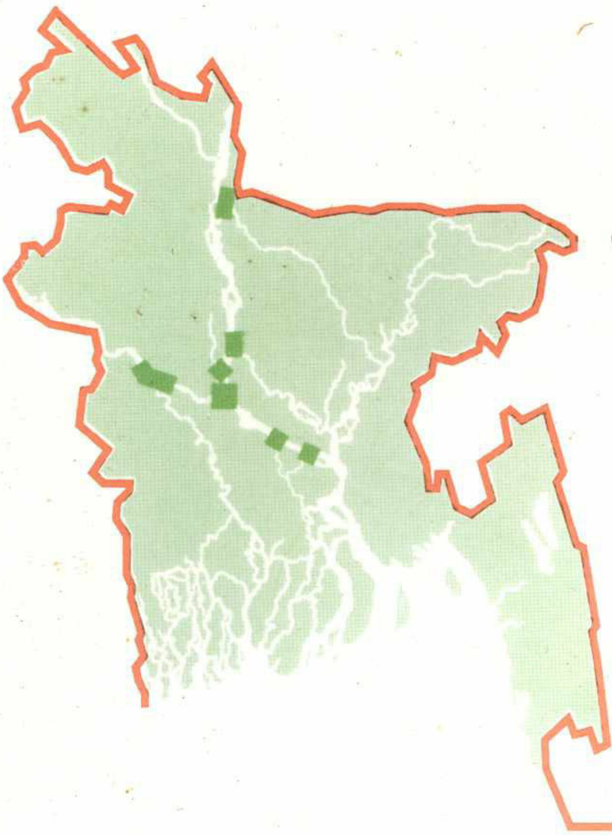

DELFT HYDRAULICS
DANISH HYDRAULIC INSTITUTE
OSIRIS
HYDROLAND
APPROTECH

Project ALA/90/04 — Commission of the European Communities

Remote sensing for morphological assessment
and
radar remote sensing pilot project

by

G.H.F.M. Hesselmans & E. Mosselman

February 1995

Contents

1 Introduction

1.1 Background

Remote sensing has proven to be a highly valuable tool for the understanding, the monitoring and the prediction of the morphological processes in the major rivers of Bangladesh. Remote sensing is therefore one of the survey techniques considered within the FAP 24 River Survey Project. In this report, the use of remote sensing for morphological assessment is discussed and a work plan for a pilot project on river bathymetry assessment by radar remote sensing is elaborated.

The objective of the pilot project is to make the technique of bathymetry assessment by radar remote sensing suited to the major rivers of Bangladesh. This is not a trivial formulation, because application to rivers is more complicated than application to coastal areas and shallow seas, where it was earlier applied successfully. Adaptations are needed in the numerical models underlying the imaging mechanism. Chapter 2 discusses the applicability of remote sensing for fluvio-morphological assessment.

Chapter 2 discusses the applicability of remote sensing for fluvio - morphological assessment. The first step in the proposed pilot project is a campaign with simultaneous measurements of bathymetry, flow field, water surface waves and radar backscatter. This is elaborated in Chapter 3. The measured data are used to test and adapt the numerical models. The resulting system is tested in a verification study and installed in Bangladesh. The feasibility for Bangladesh is assessed and recommendations are given on the use of radar remote sensing for the optimization of traditional bathymetric surveys and for a morphology early warning system. These issues are discussed in Chapter 4. Chapter 5 comprises the workplan for all these activities. Background information is given in the appendices.

1.2 Remote sensing

In its broadest sense, remote sensing includes hearing and seeing. In its more restricted operational meaning, it refers to gathering information from great distances and over broad areas, usually through instruments mounted on aircraft or orbiting space vehicles. Alternative terms for 'remote sensing' in this restricted meaning are 'earth observation' and 'teledetection'. The major advantage of remote sensing is that it provides area measurements instead of point measurements in a cheap way. Moreover, the synoptic information from area measurements allows the recognition of patterns, which is very important for the identification of relevant processes. Satellite remote sensing has the following advantages:

- *Wide area coverage:*
  The wide area coverage of satellite remote sensing offers possibilities to study large areas that are difficult to access. This is especially

important for developing countries where routine measurement programmes covering large areas are difficult to sustain. The wide area coverage also allows an evaluation of phenomena in a regional context. For instance, it is possible to correlate river channel patterns with geological features by means of an analysis of lineaments;

- *Repetitive coverage:*
  Because image-gathering satellites operate on a continuous basis, satellite remote sensing can study areas on a highly repetitive basis. This would be very costly, or impossible, to do with other survey techniques. Satellite remote sensing thus offers a unique capacity to track changes in natural phenomena;

- *Cost-effectiveness:*
  The use of satellite remote sensing data can lead to lower costs than an airborne or ground survey. Sometimes an economic optimum is obtained through combining a less dense ground survey with remote sensing; see for instance the optimization of bathymetric surveys proposed in Section 1.4;

- *Fast acquisition:*
  Satellite remote sensing data can be acquired within a shorter time frame than conventional ground-based surveys;

- *All-weather technique:*
  With conventional methods, there are usually no measurements during extreme conditions. Equipment for river measurements, for instance, may be washed away during large floods. In particular radar remote sensing is an all-weather technique, because radar radiation penetrates clouds.

Four basic classes of remote sensors can be distinguished :

- radiometers, measuring energy levels of portions of the electromagnetic spectrum;
- audiometers, measuring intensities of sound waves;
- magnetometers, measuring variations in the strength of the earth's magnetic field;
- gravimeters, measuring variations in the acceleration of gravity.

In this report only radiometry is taken into consideration. The radiometers can be subdivided into passive systems and active systems.

Passive radiometers

Passive radiometers measure radiant energy reflected or emitted by an object. Mostly, this energy falls in the visible light region (reflected) and the infrared and microwave regions (emitted). Pure emission occurs in the idealized case of 'black bodies'. A black body absorbs all radiation falling upon it, but radiates energy in a manner solely dependent upon its surface temperature. This dependence is described by Wien's law, which states that the product of surface temperature [K] and wave length of emitted radiation [m] is equal to $2.897 \cdot 10^{-3}$ Km. Hence the emission from the sun, with a surface temperature of 6000 K, is visible light, whereas emission from the earth consists of microwaves.

Active radiometers

Active radiometers use a man-made beam of wave energy as a source. This type of sensor system sends a beam of energy to an object. A part of the energy is reflected back to the source, where it is recorded by a detector. Radar remote sensing is a form of active radiometry. Brightness in a radar image is proportional to the local amount of radar backscatter. The amount of radar backscatter is a function of surface roughness. As radar radiation strikes the surface under an angle, a perfectly smooth surface would act as a mirror, reflecting all radiation away from the radar. The rougher the surface is, the more power is backscattered into the radar. There are two types of backscatter from water surfaces (as simplified cases of the full solution of the Maxwell equations):

- *specular reflection*: the water surface acts as a pure mirror at locations where its slope is such that the incidence of radiation is perpendicular to the water surface. This type of backscatter dominates at steeper angles of incidence (deviations from vertical $< 20°$);

- *Bragg scattering*: resonant scattering which occurs when water waves have the same wave length as the incident radiation, corrected for the angle of incidence. The water waves that produce this Bragg scattering are called Bragg waves. For the radar of ERS-1, their wave length is about 0.06 m. The Bragg waves on the water surface contain information on other phenomena. For instance, a long wave can be distinguished because (1) Bragg waves are observed under different angles, and (2) surface currents related to the orbital motion cause a Doppler shift in observed locations (the 'train-off-track' phenomenon).

Radar is generally used between 15 and 300 mm (1 and 20 GHz). Larger frequencies are affected by atmospheric disturbances and produce technological problems. Smaller frequencies require large antennas, and give conflicts with other telecommunications.

The types of radiation in the electromagnetic spectrum are listed in Table 1.1. The near infra-red band gives the best contrast between water and land and offers therefore the best basis for the determination of bank lines. Maximum transparency of water bodies is obtained in the yellow band of visible light. The yellow band is therefore most suited for the detection of shallow areas and relative concentrations of suspended sediment. However, the yellow band is also highly affected by atmospheric effects. The water vapour band is a thin cirrus cloud detector.

Class	Wave length	Name
Gamma rays < 0.03 Å	< 0.03 Å	Gamma rays
X-rays 0.03 - 100 Å	0.03 - 0.6 Å 0.6 - 100 Å	Hard X-rays Soft X-rays
Ultraviolet 100 - 4000 Å 0.01 - 0.4 μm	0.3 - 0.4 μm	Near ultraviolet
Visible light 0.4 - 0.7 μm	0.4 - 0.43 μm 0.43 - 0.49 μm 0.49 - 0.53 μm 0.53 - 0.58 μm 0.58 - 0.63 μm 0.63 - 0.7 μm	Violet Blue Green Yellow Orange Red
Infrared 0.7 - 300 μm	0.7 - 1.0 μm 1 - 20 μm 6 - 7 μm	Near infrared Thermal infrared (emitted rather than reflected) Water vapour band
Microwaves 0.3 - 10 mm	0.3 - 10 mm	Microwaves
Radar 1 mm - 1 m	1 - 10 mm 10 - 100 mm 100 - 1000 mm 27 - 52 mm 52 - 71 mm 71 - 194 mm 194 - 769 mm 769 - 1176 mm	EHF = Extremely High Frequency SHF = Superhigh Frequency UHF = Ultrahigh Frequency X-band C-band S-band L-band P-band
Television and radio > 1 m	1 - 10 m 10 - 100 m > 100 m	VHF = Very High Frequency HF = High Frequency LF = Low Frequency

Table 1.1 Types of radiation in the electromagnetic spectrum.

The propagation speed of electromagnetic waves is 300 000 km/s ('the speed of light'). With this value, one can easily calculate the frequencies of a certain radiation band from the wave lengths given in Table 1.1. For example, a wavelength of 57 mm (radar C-band) corresponds with a frequency of 5.3 GHz.

The level of detail of radiometric data has four dimensions and corresponding resolutions. This is shown in Table 1.2. An overview of satellites with radiometric sensors is given in Table 1.3. Sensors with a resolution of more than 100 m have not been taken into consideration. More information on satellites and sensors is given by Peters (1993).

Type	Dimension	Resolution
spatial	number of rows and columns	pixel size
radiometric	number of numerical values of pixels (e.g. 256)	levels of intensity
spectral	number of spectral bands	width of spectral bands
temporal	number of repeat observations of target	time between observations

Table 1.2 Dimensions and corresponding resolutions of radiometric data.

Satellite	Sensor	Spectral band		Spatial resolution [m]
		Name	Range [μm]	
Landsat	MSS	Landsat 1,2,3 / Landsat 4,5		
		4 / 1	0.5 - 0.6	80
		5 / 2	0.6 - 0.7	80
		6 / 3	0.7 - 0.8	80
		7 / 4	0.8 - 1.1	80
	TM	TM 1	0.45 - 0.52	30
		TM 2	0.53 - 0.61	30
		TM 3	0.62 - 0.69	30
		TM 4	0.78 - 0.91	30
		TM 5	1.57 - 1.78	30
		TM 6	10.42 - 11.66	120
		TM 7	2.08 - 2.35	30
MOS	MESSR	1	0.51 - 0.59	50
		2	0.61 - 0.69	50
		3	0.72 - 0.80	50
		4	0.80 - 1.1	50
SPOT	HRV in multispectral mode	1	0.50 - 0.59	20
		2	0.61 - 0.69	20
		3	0.79 - 0.90	20
	HRV in panchromatic mode	-	0.50 - 0.90	10
ERS-1	AMI in SAR mode	C-band	57 000	30

Tabel 1.3 Satellite-mounted sensors with spatial resolution below 100 m.

2 Applicability of remote sensing for fluvio-morphological assessment

2.1 Introduction

Collection of field data is a major element for the understanding, the monitoring and the prediction of river behavior. It usually requires a lot of means and manpower, in particular for large river systems. Routine measurement programmes are therefore still difficult to sustain in many developing countries. Time series of measurements may contain large gaps in the flood seasons when equipment is washed away. Remote sensing offers a cost-effective alternative and is not affected by the severity of floods.

Simulations with mathematical models are another major element for the understanding, the monitoring and the prediction of river behavior. River data are necessary to calibrate model parameters in the development phase, but also to update the model continuously in the operational phase of river monitoring and river management. By combining digital remote sensing imagery with mathematical models, the behavior of a river can be forecasted.

There are several applications of remote sensing to rivers. Examples are rainfall-discharge predictions based on cold-cloud duration observations, sediment yield assessment based on observations of land use and landslides in mountainous areas, river flood monitoring (real-time forecasting) and impact analysis (inundation areas, damage assessment), surface water temperature detection (industrial cooling water releases), detection of seepage through embankments during floods, etc. In this report only applications related to river morphology are addressed. The pertinent quantities are bank-line positions (land-water separation), bathymetry, floodplain topography, current pattern (flow velocity field) and sediment transport. They are discussed in the following sections.

2.2 Land-water separation

The separation between land and water can be detected by optical as well as radar remote sensors. The best contrast is found in the near-infrared band. Land-water separation with radar is based on the differences in surface roughness between water and land. This is not a matter of differences between average roughness values, but a matter of differences in the variance of roughness values. A successful example of land-water separation in the Jamuna river by means of radar is presented in Appendix B.

2.3 Bathymetry

Electromagnetic radiation is partly or, depending on the wave length, fully reflected by the water surface. Therefore, it is useful to make a distinction between bathymetry and floodplain topography, though both terms refer to the topography of the river bed. Of course it is difficult to distinguish between the two in rivers where bars and chars with different elevations can emerge from the water level during part of the year. The boundaries between the submerged and the exposed parts of the river bed change continuously (cf. Peters, 1993). Nevertheless, the distinction is useful because submerged and exposed parts of the river bed require different survey methods.

An additional difference between bathymetry and topography is the way in which they are usually mapped. Topography is usually represented by elevations with respect to a horizontal datum, whereas river bathymetry is usually represented by depths with respect to a sloping plane, e.g. the water level for a certain specified constant discharge.

The bathymetry of shallow water can be observed with passive optical remote sensing if the water is clear. In the Northsea in Europe, for instance, depths up to 10 m maximum have been determined optically with an accuracy of about 0.5 m. The best results are obtained when using wave lengths between 0.5 and 0.6 μm (yellow light). Differences in water depth are represented by differences in spectral intensity. The spectral intensity, however, is also affected by suspended sediment and haze, so that the method is mainly qualitative.

Bathymetry Assessment system

A more precise quantitative assessment of bathymetry is possible with (active) radar remote sensing, because radar is affected neither by clouds nor by suspended sediment. The technique of bathymetry assessment by radar remote sensing is operational for coastal areas and shallow seas (see Appendix C), but is also expected to have a high potential for large rivers like the Jamuna, the Ganges, the Meghna and the Padma in Bangladesh. At first glance it may seem strange that radar can be used for the assessment of bathymetry, since radar radiation is fully reflected by the water surface. The observation, however, is not direct but indirect, based on wave-current interactions at the water surface.

Variations in bed level produce modulations in surface flow velocities. The latter cause variations in the spectrum of water surface waves and hence variations in water surface roughness. Radar backscatter is a function of this surface roughness. This chain of relationships implies that the bathymetry can be assessed by a data assimilation technique, starting from an assumed bathymetry. Numerical models for (1) water flow, (2) generation and advection of waves and (3) radar backscattering are used to compute a corresponding radar image. Evaluation of the differences between the simulated radar image and the real radar image reveals the required adjustments of the assumed bathymetry. A new radar image is computed in the same way from the adjusted bathymetry and this whole procedure is repeated until the differences between the simulated and the real image are smaller than a prescribed accuracy level. The bathymetry thus obtained is approximately equal to the real bathymetry.

Another technique for bathymetry assessment by active remote sensing is the use of laser. This is still in an experimental stage and, being a form of optical remote sensing, only applicable in clear water.

Wave-current interactions can also be used for a qualitative assessment of bathymetry by optical remote sensing. Optical backscatter of solar radiation (sun glint) can locally produce similar results as radar backscatter. This is for instance visible in aerial photographs of the Brahmaputra-Jamuna River taken in 1990. Overlap areas are present on pairs of successive photographs taken only a few seconds apart. The area is often bright on one photograph due to sun glint, but of normal intensity on the other photograph because of the different angle of incidence. The bright reflection from the water surface displays submerged bed patterns that are not visible on its neutral counterpart. However, a quantitative assessment is not possible in this way and even a qualitative assessment is not feasible because only a small part of each photograph exhibits sun glint. The strong dependence on the angle of incidence makes that sun glint is less likely to appear on satellite images, because they are taken with a narrower range of incidence angles than aerial photographs.

2.4 Floodplain topography

Aerial photographs and satellite images are basically two-dimensional, whereas floodplains are essentially three-dimensional. The three-dimensional structure of floodplains determines the flow patterns during floods and hence also the pathways of sediments which are eroded from the top of the floodplains. It is possible, however, to derive three-dimensional information from photographs or images.

Photogrammetry can be used to map the topography of islands and floodplains from pairs of aerial photographs. Aerial photographs have the additional advantage of a higher resolution than satellite images. For civil applications, satellite images with better resolutions than 10 m are not tolerated by the military superpowers. In Bangladesh, institutional problems related to military security severely limit the use of aerial photography. Pursuing the operationalization of this technique for the understanding, the monitoring and the prediction of river behavior is therefore not recommended.

Another way to determine the topography of floodplains is to derive elevation contours from inundation boundaries on a series of images, taken at different water levels. However, this would require several images in a relatively narrow time window during the rising and the falling limb of the hydrograph, while overpass intervals of satellites are usually in the order of two or three weeks. Moreover, obstructions on the floodplains may back up water locally, producing more inundations, and may prevent water from flowing into low-lying areas elsewhere.

In 1993, the possibility to determine the topography of sand bars by deriving the elevation of the sand surface above groundwater level from infrared observations of soil moisture was discussed in FAP 24. However, the idea was then abandoned because it involved too many uncertainties and seemed less suited for the vegetated parts of floodplains.

Pairs of radar images can be used for topographic mapping through the technique of radar interferometry (Zebker & Goldstein, 1986; Hirosawa & Kobayashi, 1986; Gabriel & al, 1989). There are, however, some problems which make the applicability to islands and floodplains in the rivers of Bangladesh questionable:

- The accuracy depends on vegetation. The effect of vegetation is negligible or absent in mountains and on ocean surfaces, but considerable on the relatively flat islands and floodplains
- The accuracy is affected by atmospheric perturbations
- Successful application of the technique requires a high correlation between the two images, which is not ensured when the two images are taken several weeks apart.

In conclusion, photogrammetry based on aerial photography seems technically the best remote sensing method to assess floodplain topography, but its application in Bangladesh is hampered by institutional problems.

2.5 Flow velocity field

Streamlines and hence flow patterns are visible on optical images (SPOT) and radar images (ERS-1) of the major rivers in Bangladesh. On the SPOT images, the streamlines are visualized by elongated plumes of suspended sediment. On the ERS-1 images, the streamlines are visualized by elongated areas of constant flow velocity, in particular by very bright zones which represent high flow velocities. These synoptic flow patterns give a good insight into the processes in the river. They are also useful for the calibration of numerical models. The advantage of SPOT images over ERS-1 images is that SPOT images are easier to interpret. They are less speckled, and the imaging mechanism is more or less the same as in the human eye. The advantage of ERS-1 images is that they allow a quantification of flow velocities through the Bathymetry Assessment System described in Section 2.3.

2.6 Suspended sediment and mixing

Optical remote sensing offers the best opportunities to observe relative concentrations of suspended sediment and related phenomena such as mixing. Like for bathymetry observation, the best results are obtained when using wave lengths between 0.5 and 0.6 μm (yellow light). An excellent illustration is formed by SPOT-Map sheet 79 I11 of 13 October 1994. This sheet shows the confluence of the Padma and the Meghna rivers. In fact several rivers join in this area, each with its own sediment concentration or type of sediment. The interfaces between the waters from different tributaries are clearly discernible and show a wave pattern which corresponds to the large turbulent eddies at the interfaces.

The spectral intensity, however, is not only related to the sediment concentration, but also to the type of sediment (mineral composition), the water depth and the presence of haze. This means that a quantification of suspended sediment concentrations on the basis of SPOT images still requires a lot of additional ground truth information.

In principle, radar remote sensing can not be used to observe sediment concentrations, because radar radiation is fully reflected by the water surface and wave patterns are only influenced by suspended sediments when the concentrations are extremely high. It might be possible, however, to correlate higher sediment transports with zones of higher turbulence, which could be detected at the water surface.

2.7 Morphological predictions

The objective and corresponding time span of morphological predictions determine which type of remotely sensed data is most useful. Predictions spanning a few weeks or months are needed for construction works (e.g. Jamuna bridge, FAP 21 test structures) and the positioning of navigation buoys. They require a high level of detail and aerial photography and high-resolution SPOT imagery provide the best information for this purpose. Predictions more than one year ahead are needed for, for instance, site selection for structures and early anticipation of developments, which are to be altered by recurrent measures. Then images from LANDSAT and MOS are more useful, because the morphological system of the major rivers in Bangladesh exhibits deterministic chaos (Klaassen & al, 1993) and this deterministic chaos implies that the consideration of a sufficiently long river reach (and a probabilistic approach) is more determining for the quality of the predictions than the use of a high level of detail. Quite a lot of practical applications require morphological predictions more than one year ahead.

Sometimes rough indicators are sufficient for even short-term predictions. That is the case when only the general changes of the channel pattern in the river need to be monitored. Examples of such rough indicators are the detection of positions and alignments of main channels and, on the ground, the measurement of water surface slopes at carefully selected locations (Peters, 1981; Peters & Wens, 1991).

2.8 Motivation of pilot project

The following problems pose limits to the applicability of remote sensing:

- The earth surface can be invisible due to clouds, which are ubiquitous in Bangladesh during the flood season when the major portion of the morphological changes occurs. This is a problem for the traditional optical and infrared remote sensing, but not for radar remote sensing. Radar radiation penetrates clouds.

- Sediment concentrations can reduce the visibility of submerged river beds. However, radar backscatter from a water body is not affected by turbidity.

- Aerial photographs and satellite images are basically two-dimensional, whereas river beds are essentially three-dimensional. There are several ways, however, to derive three-dimensional information from photographs or images. Photogrammetry can be used to map the topography of islands and floodplains from pairs of aerial photographs. Institutional problems, however, severely limit the use of aerial photography in Bangladesh. Another way is to derive elevation contours from inundation boundaries on a series of images, taken at different water levels. Finally, there are special radar remote sensing techniques for bathymetry assessment and topographic mapping.

The analysis of these problems shows that radar remote sensing can be a powerful tool. It penetrates clouds, is not affected by turbidity and can be used to assess the three-dimensional shape of river beds.

River bathymetry assessment by radar remote sensing would greatly enhance three major applications:

- *Optimization of traditional bathymetric surveys:*
  The quick synoptic and relatively cheap survey with remote sensing offers a possibility to optimize a combination of remote sensing and traditional survey methods. The reduction of costs would be valuable in particular because the expensive traditional survey methods are often not sustainable in low-income countries.

- *Study of morphological processes:*
  The synoptic observation of morphological changes during a flood serves the central objectives of the River Survey Project FAP 24.

- *Early warning system for undesired river planform changes:*
  The monitoring of morphological changes during a flood would be a valuable support for the operation of the recurrent measures proposed under FAP 22.

The idea to assess the bathymetry of rivers in Bangladesh with radar remote sensing was explained and discussed within FAP 24 in 1992 and presented during the International Workshop on the Morphological Behavior of the Major Rivers in Bangladesh, held in Dhaka in November 1993 (Mosselman & Wensink, 1993, see Appendix D). It resulted in the decision to carry out a pilot project within the framework of the FAP 24 River Survey Project (topic 9.5 in letter RSP/3.7/998 to FPCO).

The radar image of the confluence of the Jamuna and the Ganges in Figure 2.1 shows that backscatter patterns do have a relation with current patterns in the rivers, so that application to the major rivers in Bangladesh seems promising. A more detailed analysis of what can be seen on that radar image is given in Appendix B.

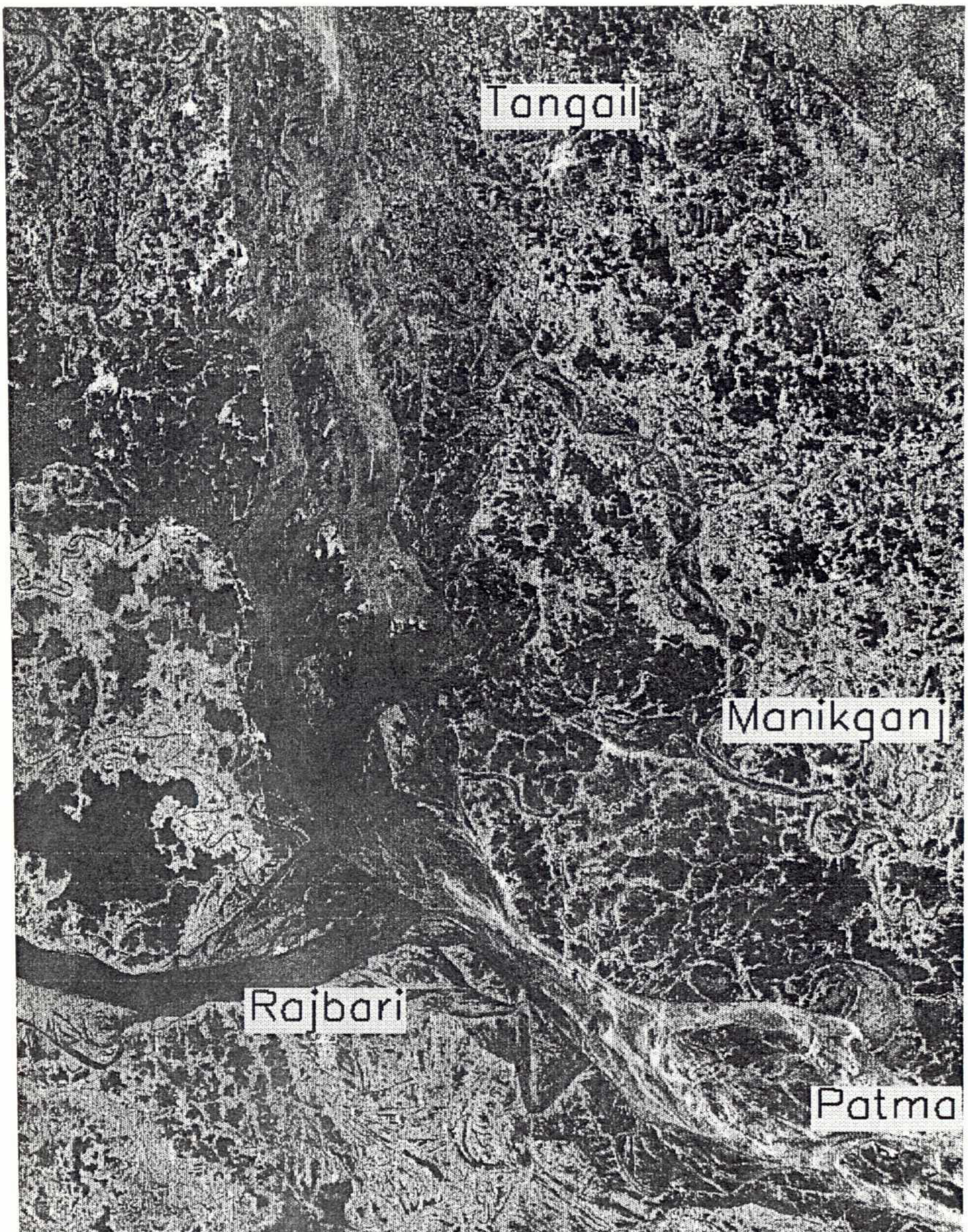

Fig. 2.1 ERS-1 image of the confluence of the Jamuna and Ganges Rivers.

3 Measurement campaign

3.1 General

The proposed pilot project starts with a measurement campaign in which radar backscatter, bathymetry, flow field and water surface waves are measured simultaneously. Wind speed, wind direction, air temperature and water surface temperature are measured as well, because they govern the generation of waves. The radar backscatter is measured from the ERS-1 and ERS-2 satellites, the other quantities from two FAP 24 survey vessels. Rain is registered if it disturbs the water surface during satellite overpass.

The measurement campaign would take two weeks during the 1995 flood season. It would cover a 20×10 km^2 area near Bahadurabad, between BTM northings 2770 and 2790, see Figure 3.1.

Data from only a part of the area would be used for the adaptation of the underlying numerical models. The data from the remainder of the area should be used for the verification study.

The radar measurements cover the whole area and recording takes less than a minute. The field measurements are collected along section lines about 200 m apart. By using a DGPS the position of each vessel can be monitored with an accuracy of 5 m.

3.2 Radar backscatter

Synthetic aperture radar (SAR) images of the project area will be collected during each overpass of an ERS-1 or ERS-2 satellite in the campaign period. In two weeks about 3 to 5 images of the area can be recorded. ERS precision SAR images have a pixel size of 12.5×12.5 m^2, a resolution of 30 m and cover an area of 100×100 km^2.

3.3 Bathymetry

The bathymetry in the area will be measured with an Acoustic Doppler Current Profiler (ADCP) and/or a dual-frequency echosounder. Depths are sounded once per second. This results in a sampling interval of 1.5 m for a ship velocity of about 3 knots. The depth accuracy is better than 0.20 m., when combined with slope measurements. Depth measurements are reduced to Standard Low Water (SLW).

3.4 Flow field

Flow velocities and directions will be measured along each sailed track at intervals of 6 seconds. An Electromagnetic Flow Meter (EMF) is used to measure the flow at a depth of 1.0 m, whereas the ADCP is used to measure the flow at depth intervals of 0.5 m, starting 2.7 m below the surface and

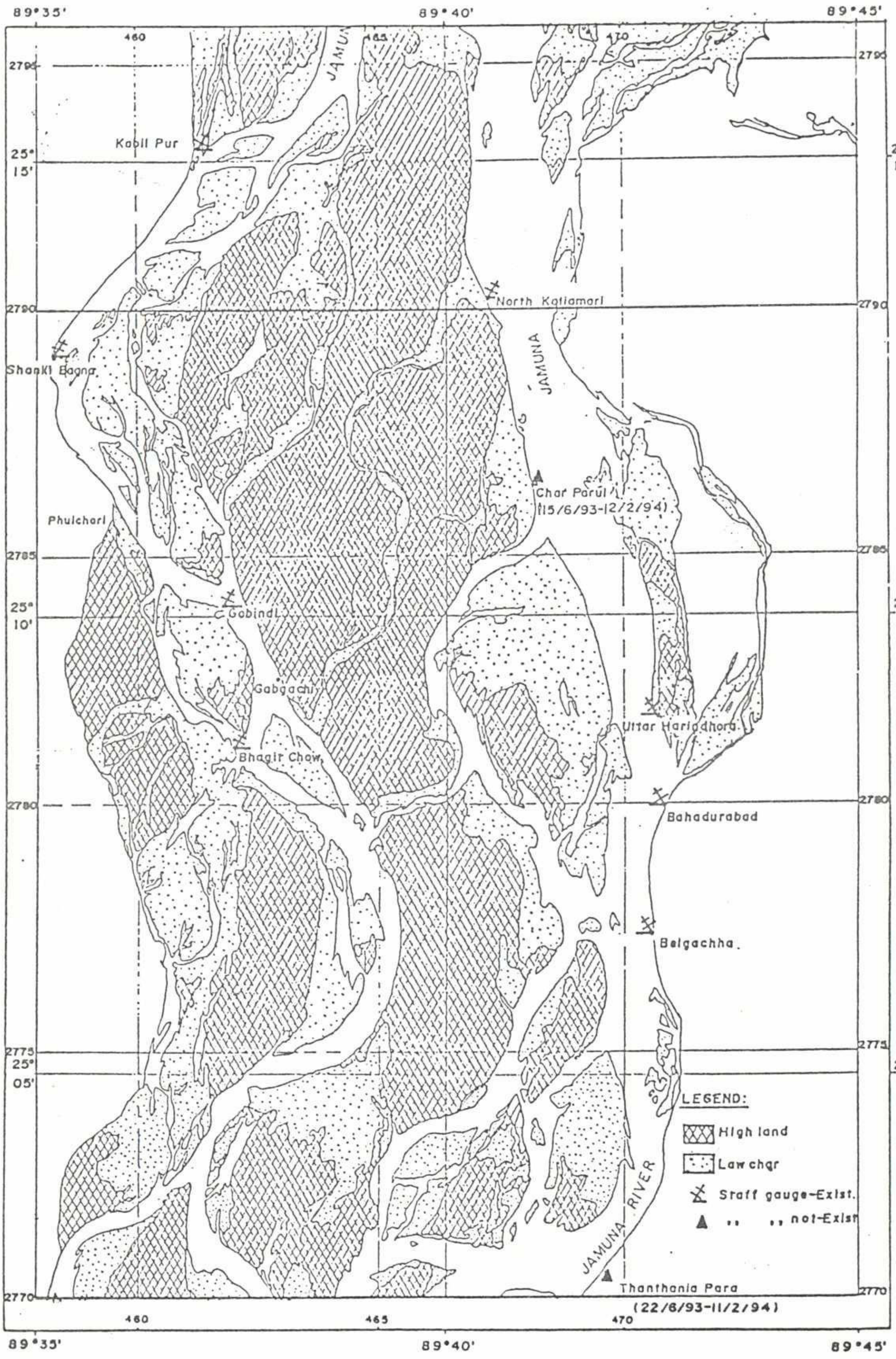

Figure 3.1 : Pilot project area

ending 0.5 m above the river bed. The measuring accuracy is about 0.1 m/s. Depth-averaged flow velocities and directions are derived from the measurements.

3.5 Water surface roughness

The water surface roughness is produced by two types of waves, wind waves and waves produced by high flow velocities. The wind waves can be measured directly or be calculated from measured wind and temperature data (see Sections 3.6).

The Bragg waves are the relevant waves on the water surface, because radar backscatter is proportional to the water surface wave energy at the Bragg wave length. They are defined as the waves which have the same wave length as the radar radiation, corrected for the angle of incidence. For a radar wave length of 30 mm and an incidence angle between 17° and 30°, the Bragg wave length varies between 0.05 and 0.25 m. This is the range of interest for measurements. There are no generally accepted procedures to measure these short (capillary) waves under varying flow conditions. For wind waves, standard relations hold between the energy densities at different wave lengths, so that the energy near the Bragg wave length can be derived from wave measurements at other wave lengths. As yet, however, no such standard relations are known for flow-driven waves.

Different characteristic wave conditions will be recorded by video. Oral comments indicating time and position are added while recording. A staff gauge with clear elevation marks will be mounted on a cantilevered beam from the vessel. The video must zoom in on the water level at the gauge, but also zoom out to give an overview of the water surface pattern.

3.6 Climatological parameters

The air and water surface temperatures will be measured at the moments when the radar images are recorded. The difference between these temperatures influences the effect of wind on the roughness of the water surface. If the water is warmer than the air, the air-water interface becomes unstable. As a consequence, the water surface becomes rougher than it would be for the same wind speed under normal conditions.

Wind speeds and directions should be recorded at five-minute intervals starting one hour before and ending one hour after satellite overpass.

Rain is registered if it disturbs the water surface during satellite overpass.

4 Adaptation and operationalization of the Bathymetry Assessment System

4.1 Introduction

The imaging mechanism in the Bathymetry Assessment System is based on numerical models for (1) water flow, (2) generation and advection of waves and (3) radar backscattering. These models have proven to perform well in shallow seas (Vogelzang & al, 1992), the coastal waters of Belgium and The Netherlands (Hesselmans & al, 1994) and the coastal waters of Germany (Hesselmans, 1994; see Appendix C). The major rivers of Bangladesh, however, involve the following additional problems:

- The geometries are more complex. The efficiency of the computations can then be substantially improved by formulating the models in a curvi-linear boundary-adapted coordinate system.
- The flow fields are more complex. Hence some of the simplifications used for coastal areas and shallow seas are no longer justified.
- The water surface roughness is not only a result of wind waves. High flow velocities produce waves as well.
- There is no data infrastructure for radar remote sensing in Bangladesh.

The first two problems can be solved simply by using an advanced 2D flow model, several of which are operational. The third problem requires seemingly an adaptation of the wave model, but this is analyzed in Section 4.2. The last problem is addressed in Section 4.5. No particular problems are expected with the radar backscatter model.

4.2 Model adaptation

Waves in coastal areas and shallow seas are generated by the wind. Modulations in their spectrum due to flow velocity variations can be modelled with the action balance equation, using a relaxation term to simulate the restoring forces of wind input and wave breaking.

In the Jamuna River, high flow velocities generate waves as well. It seems that there is no model for these flow-generated waves. A short literature search of studies on flow-generated waves will be carried out to verify and substantiate this statement. One might conclude that it is hence necessary to establish an empirical relation between wave data and flow data, as well as an empirical relation between wave data and radar backscatter because standard relations for wind-generated waves may not apply. However, it is more practical then to establish a direct empirical relation between surface flow velocities and radar backscatter, without the intermediate step of the wave data. This empirical relation is to be induced from measurements in the river.

4.3 Verification study

Only data from a part of the project area will be used for the adaptation of the numerical models. The data from the remainder of the area will be used for the verification study in Bangladesh. The verification study would be carried out by image processing specialists of SPARRSO under the supervision of an expatriate radar remote sensing specialist of FAP 24.

4.4 Technology transfer

The supervised execution of the verification study by image processing specialists of SPARRSO would serve as an on-the-job training. A broader dissemination of knowledge on the possibilities and limitations of the technique could be pursued within the framework of the FAP 24 training programme.

4.5 Data infrastructure

Operational applications require an early availability of remotely sensed radar data. This means that a good connection with the ERS ground station of the Thailand Remote Sensing Center in Bangkok must be established. A possible future alternative is that radar satellite data are received at SPARRSO or at the regional ground station at the Atomic Energy Research Establishment in Savar, Bangladesh. The feasibility of such arrangements would need to be assessed.

5 Work plan

5.1 Work break-down

5.1.1 Introduction

The activities of the project are grouped in eight distinct work packages. They are described below. The work packages 2, 3 and 4 are recommended to be executed in the Netherlands for reasons of available computer infrastructure and short communication lines with various specialists in related fields. Execution in Bangladesh is also possible, but requires extra costs for setting up a suitable computer infrastructure (see Appendix A) in Bangladesh and for explicit backstopping by the specialists in related fields.

5.1.2 Work package 1: Measurement campaign

The measurement campaign consists of the following activities:

1.1 Mobilization
1.2 Measurements during survey according to standard procedures of FAP 24, including quality assurance
1.3 Writing of survey report, which includes: description of survey area, positions of measured transacts, outline of survey data, description of the digital data format
1.4 Acquisition of ERS SAR images
1.5 Writing of report on the remote sensing data and the hydro-meteorological conditions during image acquisition. The latter bears on the operational feasibility of the method. Hard copies of the relevant part of the satellite image will be included and the quality of the image will be verified.

5.1.3 Work package 2: Model adaptation

The adaptation of the model consists of the following activities:

2.1 Flow model:
- Development of a 2D-flow model for the test area.
- Comparison of flow measurements with model predictions
- Adaptation of the model, if necessary

2.2 Radar backscatter model:
- Short literature search of studies on waves produced by high flow velocities
- Induction of an empirical relation between radar back scatter and flow data (flow velocities, flow gradients etc.) from the measurements

- Implementation of an empirical model for radar backscatter

2.3 Interfacing of the models, with adaptation of data assimilation procedure

2.4 Testing, using data from a part of the project area

2.5 Writing of progress report, which includes: description of the bathymetry assessment system, the modifications and the test results.

5.1.4 Work package 3: Testing of model performance

The testing of model performance consists of the following components:

3.1 Channel detection:
- Assessment of the visibility of channels in the SAR imagery. Interpretation of ambiguities will be resolved by using SPOT images
- Determination of differences in channel position on subsequent ERS SAR images

3.2 Survey optimization:
- Generation of bathymetric maps based on ERS SAR data and subsets of the survey data
- Assessment of the accuracy of these "limited survey" maps

3.3 Writing of progress report on test results.

5.1.5 Work package 4: Software update

The updating of the software consists of the following activities:

4.1 Adaptation of software for input, output and presentation to the BTM (Bangladesh Transverse Mercator) coordinate system
4.2 Writing and updating of software documentation and user manuals.

5.1.6 Work package 5: Installation of software in Bangladesh

5.1 Selection of the organization and location where the software is to be installed.
5.2 Installation.

5.1.7 Work package 6: Transfer of knowledge

Knowledge will be transferred through a six-day course and on-the-job training for about four Bangladeshi experts. The knowledge transfer comprises the following activities:

6.1 Preparations

6.2 Introductory course, comprising:
- background theory
- presentation of survey measurements, SAR data (see work package 1)
- presentation of previous results (see activities 2.4, 3.1 and 3.2)
- introduction to software, manuals and documentation

6.3 On-the-job training and case study
- getting started: reading, writing, plotting, inspecting data, etc.
- reproduction of results obtained in work package 3
- processing of remaining part of survey data.

5.1.8 Work package 7: Verification

A verification is carried out by evaluating the results of the case study.

5.1.9 Work package 8: Final report

This final report will present the results of the project and provide recommendations on the operational use. In particular, a detailed description of the way in which radar remote sensing can be used to optimize traditional bathymetric survey methods will be elaborated.

5.2 Required input and time planning

A tentative estimate of the required number of manmonths is given in Table 5.1. The time planning is shown in Figure 5.1. The decision on the precise period of the measurement campaign should be taken early 1995 when the final orbits of the ERS-1 and ERS-2 satellites are known, as well as the availability of the survey vessels. An acquisition request should be sent to ESA as soon as the campaign period has been selected, in order to ensure the recording of SAR images. The data would be acquired through the ERS ground station of the Thailand Remote Sensing Center in Bangkok.

The available resources of FAP 24 do not allow execution of all these work packages within the frame-work of the River Survey Project. Additional funding needs to be sought

Work package	Description	Country	Manmonths	
			expatriate specialist	local specialist
1	Measurement campaign	Bangladesh	1*	1*
2	Model adaptation	The Netherlands	2	2
3	Testing of model performance	The Netherlands	2	2
4	Software update	The Netherlands	1	
5	Installation of software in Bangladesh	Bangladesh	1	1
6	Transfer of knowledge	Bangladesh	1	1**
7	Verification	Bangladesh	1	2
8	Final report	Bangladesh	1	1
Total			10	10

** not including time of trainees
* survey crew not included

Table 5.1 : Required manmonths for work packages (tentative)

Additional expenses are:

- three to five ERS images, costing about US$ 800,- each
- two SPOT images
- computers
- PC-WAVE licence
- reproduction of reports
- travel and subsistence

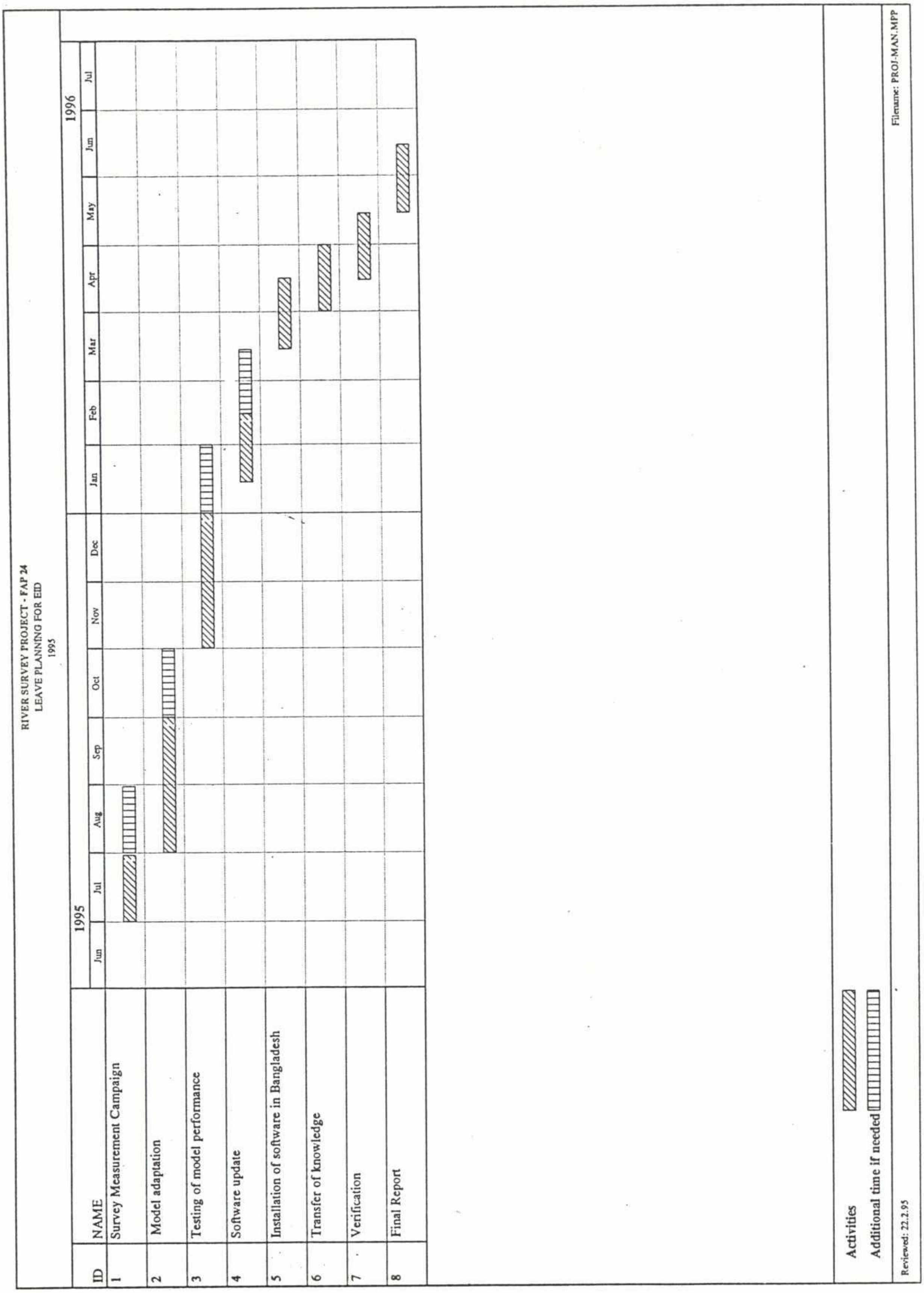

Figure 5.1 : Time planning.

5.3 Products

Reports are produced and results and data are made available after each work package. They are specified below.

Work package 1, measurement campaign:

- Survey report, with all measured data, data formats, measurement procedures, weather conditions (wind, rainfall, temperature) and scale 1:20,000 maps showing transacts sailed, river banks and bathymetry.

- Survey data in digital format:
  - bathymetry: x,y,z,t
  - flow vector: x,y,z,t,u,v,w
  - wind vector: x,y,z,t,U,φ
  - temperature: x,y,z,t,T_{air},T_{water}
  - river bank: x,y,t
  - water level: x,y,z,t

  where:

  x = easting in BTM
  y = northing in BTM
  z = depth or elevation
  u,v,w = components of flow vector
  U = wind speed
  φ = wind direction
  T_{air} = air temperature
  T_{water} = water temperature

- Video tape recording of wave conditions.

- Remote sensing report, with description of the acquired SAR images and hard-copies of the relevant part of the images. The hydro-meteorological conditions will be discussed in relation to the conditions in Bangladesh in general.

- Remote sensing data: all the acquired ERS data.

Work package 2, model adaptation:

- Progress report, with a description of the flow and radar backscatter models in the River Bathymetry Assessment System. The adaptations of the models are explained and the results of the tests are presented, with an assessment of the accuracy.

Work package 3, testing of model performance:

- Test report, with a discussion of the potential of the system for optimization of traditional bathymetric surveys and channel detection in a morphology early warning system.

Work package 4, software update:

- Software, adjusted to the major rivers in Bangladesh
- Documentation and user manuals

Work package 5, installation of software in Bangladesh:

- Bathymetry assessment system installed on a suitable computer system in Bangladesh. In view of future hardware and software developments it is recommended to postpone the selection of the hardware.

Work package 6, knowledge transfer:

- Introductory course and on-the-job training

Work package 7, verification:

- Case study report

Work package 8, final report:

- Final report, with conclusions on the technical and operational feasibility of the system and recommendations for the optimization of traditional bathymetric survey methods and a morphology early warning system.

Remarks :
The main purpose of the pilot project is to demonstrate the feasibility of the River Bathymetry Assessment system, based on radar imagery. For this pilot project a standard available 2D flow model will be used. Regular application of the system may however benefit from a simplified 2D - model, to facilitate rapid routine application of the system. The development of such simplified 2D - flow model is not part of this pilot project.

References

Gabriel, A.K., R.M. Goldstein & H.A. Zebker (1989),
Mapping small elevation changes over large areas: Differential radar interferometry.
J. Geophys. Res. - Oceans, Vol.94, No.7, pp.9183-9191.

Hesselmans, G.H.F.M. & E. Mosselman (1994),
ERS-1 to monitor morphological changes and flooding in Bangladesh.
Rep. H1221, DELFT HYDRAULICS.

Hesselmans, G.H.F.M. (1994),
Seabed bathymetry February 1994, Area A1 SAR-survey.
Rep. H1900, DELFT HYDRAULICS.

Hesselmans, G.H.F.M., G.J. Wensink, C.J. Calkoen & H. Sidhu (1994),
Application of ERS-1 SAR data to support the routing of offshore pipelines.
Rep. H1787, DELFT HYDRAULICS.

Hirosawa, H. & N. Kobayashi (1986),
Terrain height measurement by synthetic aperture radar with an interferometer.
Int. J. Remote Sensing, Vol.7, No.3, pp.339-348.

Klaassen, G.J., E. Mosselman & H. Brühl (1993),
On the prediction of planform changes in braided sand-bed rivers.
Adv. in Hydro-Sci. and -Engrg., Ed. S.S.Y. Wang, pp.134-146.

Mosselman, E. & G.J. Wensink (1993),
River bathymetry observation with radar remote sensing.
Int. Workshop Morphol. Behaviour of the Major Rivers in Bangladesh, Dhaka.

Peters, J.J. (1981),
Water and sediment gauging of the Zaïre (Congo).
Proc. 19th Congress IAHR, New Delhi, Vol.2, paper A(b)-8, pp.173-182.

Peters, J.J. & F. Wens (1991),
Maintenance dredging in the navigation channels in the Zaire river inner delta.
Proc. COPEDEC III Conf., Mombasa, Sept.1991, pp.975-988.

Peters, J.J. (1993),
Content needs for SPOT images and other remote sensing, FAP 24 - River Survey Project Management Report.

Vogelzang, J., G.J. Wensink, G.P. de Loor, H.C. Peters & H. Pouwels (1992),
Sea bottom topography with X-band SLAR: the relation between radar imagery and bathymetry.
Int. J. Remote Sensing, Vol.13, No.10, pp.1943-1958.

Zebker, H.A. & R.M. Goldstein (1986),
Topographic mapping from interferometric synthetic aperture radar observations.
J. Geophys. Res. - Oceans, Vol.91, No.5, pp.4993-4999

Appendices

Appendix A

Hardware and software requirements

Hardware and software requirements

Currently the software of the bathymetry assessment system at DELFT HYDRAULICS runs on a HP710 workstation with 32 Mbyte RAM and 1.8 Gbyte hardisk. By means of a local network, the workstation is connected to peripherals, such as a colour printer and a tape reader for the satellite images. the software of the Bathymetry Assessment System is programmed mainly in a fourth-generation language. This software package is called PV-WAVE. it is available for a number of other workstations as well as for personal computers.

If the software system is implemented on a PC, the system requirements are :

- Windows 3.1 operating system
- 386 processor plus co-processor
- 640x480 8-bit display
- 8 Mbytes RAM
- 20 Mbytes available on hard disk

In addition 1 GByte on hard disk is required to store the remote sensing data and the bathymetric maps. Furthermore, the system should be part of a local area network in order to connect it to peripherals as mentioned above.

Appendix B

ERS-1 to monitor morphological changes and flooding in Bangladesh

Reprint of DELFT HYDRAULICS report H1221
by
G.H.F.H.Hesselmans & E.Mosselman (1994).

Summary

The Jamuna River is the lowest reach of the Brahmaputra River in Bangladesh. It is a large braided sand-bed river in which the morphological processes occur so rapidly that in one year time its planform is changed substantially. In 1987 and 1988 Bangladesh was struck by several floods which caused severe damage to the agricultural production and infrastructure. To accelerate the development of Bangladesh, the Flood Action Plan (FAP), was initiated. Within the FAP project existing and new projects are coordinated by the Bangladesh government and the World Bank. The main objective of the FAP project is to control flooding. DELFT HYDRAULICS is involved in several projects within the FAP framework:

- FAP 21/22 Bank protection, River Training and AFPM Pilot Project
- FAP 24 River Survey Programme.

One of the main objectives of the River Survey Programme is to collect reliable all-season hydrological, morphological and hydrographic data at key locations along the country's main river systems, with emphasis given to collection of data during the monsoon season introducing improved or new technology as appropriate (The Flood Action Plan, Bangladesh 1993).

Remote sensing technology offers new possibilities to monitor river behaviour in large inaccessible areas. This is particularly relevant for flood conditions. The extent of the floodings can be monitored as well as the serviceability of communication roads. The morphological development of a river in the horizontal plane can be assessed at low cost using multi-temporal satellite images. Based on optical remote sensing images recorded in the dry season, differences in the position of the river branches of the Jamuna river have been established from 1973 onward (Klaassen et al. 1993).

Microwave remote sensing is not hindered by cloud cover. Therefore, it offers the possibility to monitor the development of rivers during the wet season and the dry season. Synthetic Aperture Radar (SAR) imagery of Bangladesh can be recorded by the ERS-1 (the first European Remote Sensing satellite, launched in July 1991). At DELFT HYDRAULICS applications based on ERS-1 SAR data have been developed. These techniques have already been tested and applied in the North Sea and the Dutch coastal waters. The Netherlands bears some resemblance to Bangladesh: a low-lying country intersected by several rivers and a large delta.

Potential applications of SAR imagery for Bangladesh are:

- assessment of state of infrastructure (embankment, roads, etc),
- assessment of horizontal position of rivers during dry and wet season,
- assessment of flooded areas,
- assessment of local elevation contours,
- detection of sand waves and sand banks, and
- assessment of river bottom topography.

The aim of this study is to show which techniques can be applied successfully in Bangladesh. Some techniques may have to be adapted to the specific conditions found in Bangladesh.

Contents

1 Introduction

The Jamuna River is the lowest reach of the Brahmaputra River in Bangladesh. It is a large braided sand-bed river in which the morphological processes occur so rapidly that in one year time its planform is changed substantially. Local bank erosion rates can be as high as 1 km per year. Two centuries ago the river moved to its present course, a hundred km further to the west.

In 1987 and 1988 Bangladesh was struck by several floods which caused severe damage to the agricultural production and infrastructure. To accelerate the development of Bangladesh, the Flood Action Plan (FAP), was initiated. Within the FAP project existing and new projects are coordinated by the Bangladesh government and the World Bank. Furthermore 26 studies, sponsored by 17 donor countries were initiated. The main objective of the FAP project is to control flooding. DELFT HYDRAULICS is involved in several projects within the FAP framework:

- FAP 21/22 Bank protection, River Training and AFPM Pilot Project
- FAP 24 River Survey Programme.

The River Survey Programme covers locations along selected main rivers of the country: the Brahmaputra/Jamuna, Ganges, Meghna and Padma, plus the main distributaries of these rivers; the Old Brahmaputra, the Dhaleswari, the Gorai and the Arial Khan. One of the main objectives of the project is to collect reliable all-season hydrological, morphological and hydrographic data at key locations along the country's main river systems, with emphasis given to collection of data during the monsoon season introducing improved or new technology as appropriate (The Flood Action Plan, Bangladesh 1993).

Remote sensing technology offers new possibilities to monitor river behaviour in large inaccessible areas. This is particularly relevant for flood conditions. The extent of the floodings can be monitored as well as the serviceability of communication roads. The morphological development of a river in the horizontal plane can be assessed at low cost using multi-temporal satellite images. DELFT HYDRAULICS successfully used these new measurement techniques for the Jamuna River in Bangladesh. Based on optical remote sensing images recorded in the dry season, differences in the position of the river branches of the Jamuna river have been established from 1973 onward (Klaassen et al. 1993).

Microwave remote sensing is not hindered by cloud cover. Therefore, it offers the possibility to monitor the development of rivers during the wet season as well. Synthetic Aperture Radar (SAR) imagery of Bangladesh can be recorded by the ERS-1 (the first European Remote Sensing satellite, launched in July 1991). At DELFT HYDRAULICS applications based on ERS-1 SAR data have been developed. These techniques have already been tested and applied in the North Sea and the Dutch coastal waters. The Netherlands bears some resemblance to Bangladesh: a low-lying country intersected by several rivers and a large delta.

Potential applications of SAR imagery for Bangladesh are:

- assessment of state of infrastructure (embankment, roads, etc),
- assessment of horizontal position of rivers during dry and wet season,
- assessment of flooded areas,
- assessment of local elevation contours,
- detection of sand waves and sand banks, and
- assessment of river-bottom topography.

Remote sensing products yielding position estimates can be considered as stand-alone products. Quantitative products, such as depth assessments require calibration data which can only be obtained by *in situ* measurements. In the latter case remote sensing can be used to reduce the effort in bathymetric surveys.

The aim of this study is to assess which techniques can be applied successfully in Bangladesh. Some techniques may have to be adapted to the specific conditions found in Bangladesh. Note that none of the potential applications of the SAR imagery can be attained by optical remote sensing. During the wet season optical remote sensing often cannot be used because of excessive cloud cover and bathymetry may be severely hindered by high turbidity levels.

In Chapter 2 of this report the potential applications are described in more detail. Chapter 3 shows the remote sensing data and the *in situ* measurements. Chapter 4 shows the results for a selected area. In Chapter 5 the results are discussed and in Chapter 6 the conclusions and recommendations are presented.

2 Applications

In the introduction six applications were mentioned. These applications will be described in greater detail in this Chapter.

Assessment of the state of the infrastructure

The state of the infrastructure can be determined by means of visual inspection of the SAR imagery. For example places where the river embankment may be breached can thus be detected. This can be done in the dry season as well as in the wet season.

Assessment of horizontal position of rivers during dry and wet season

The horizontal position of rivers is based on a discrimination between water and land in the SAR imagery. This requires the identification of the difference in radar backscatter signature between land and water. Both signatures can be described by a local average and image texture.

Assessment of flooded areas

Detection of flooded areas requires a segmentation of the imagery in land and water. This can be done by means of the same algorithm used to determine the position of rivers.

Assessment of local elevation contours

The water surface can be considered to be locally flat. Therefore, the line separating water and land is a constant elevation contour. Determining the border between land and water for several water levels gives a set of elevation contours.

Detection of sand waves and sand banks

Under favourable meteorological and hydrodynamic conditions (moderate winds and strong currents), air- and space-borne SAR imagery show features of the bottom topography of shallow coastal waters (Alpers and Hennings 1984, Vogelzang et al. 1989). It is generally accepted that the imaging mechanism consists of three steps (for more details see Calkoen et al., 1993):

1) Interaction between current and bottom topography results in modulations in the (surface) current-velocity.
(2) Modulations in surface current-velocity cause variations in the wave spectrum.
(3) Variations in the wave spectrum cause modulations in the level of radar backscatter.

Based on this three-step mechanism a computer model has been developed, which is used to interpret radar images. This model is particularly suited to detect sand waves and sand banks oriented perpendicular to the flow direction.

Assessment of river-bottom topography

The model described above does not include turbulence. Turbulence is a common phenomenon in rivers. Especially in the main stream, where flow velocities are high. The following relation between river bottom topography and radar backscatter seems to be an acceptable working hypothesis:

(1) Flow velocity is highest in the deeper parts of the river.
(2) High flow velocities result in high turbulence levels.
(3) High turbulence levels cause increased surface roughness and high radar backscatter levels.

At the moment no information as to when this relation may be applicable is available. Furthermore, no quantitative (empirical) relation is known to us from literature.

80

3 Experimental site and available data

Bangladesh is located in South-East Asia, and its position is indicated in Figure 1.

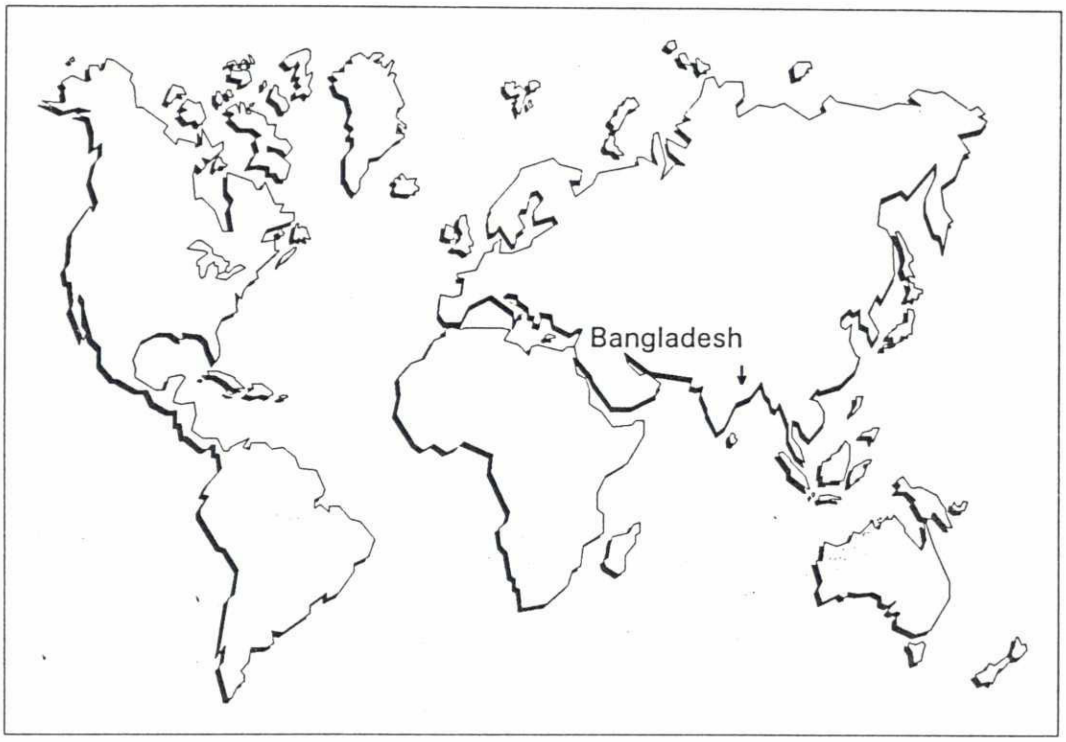

Figure 1 World map

Two ERS-1 SAR images of this country were obtained. The parameters of these images are compiled in Table 1. The two images can be linked to a single image, covering an area of 100 km x 200 km. The result is given in Figure 2.

Acquisition date	July 24, 1993 04:34 (GMT)	July 24, 1993 04:35 (GMT)
Scene centre	89.83 W 24.92 N	89.63 W 24.03 N
pixel size	12.5 m x 12.5 m	12.5 m x 12.5m
projection	UTM	

Table 1 Parameters of both ERS-1 SAR images

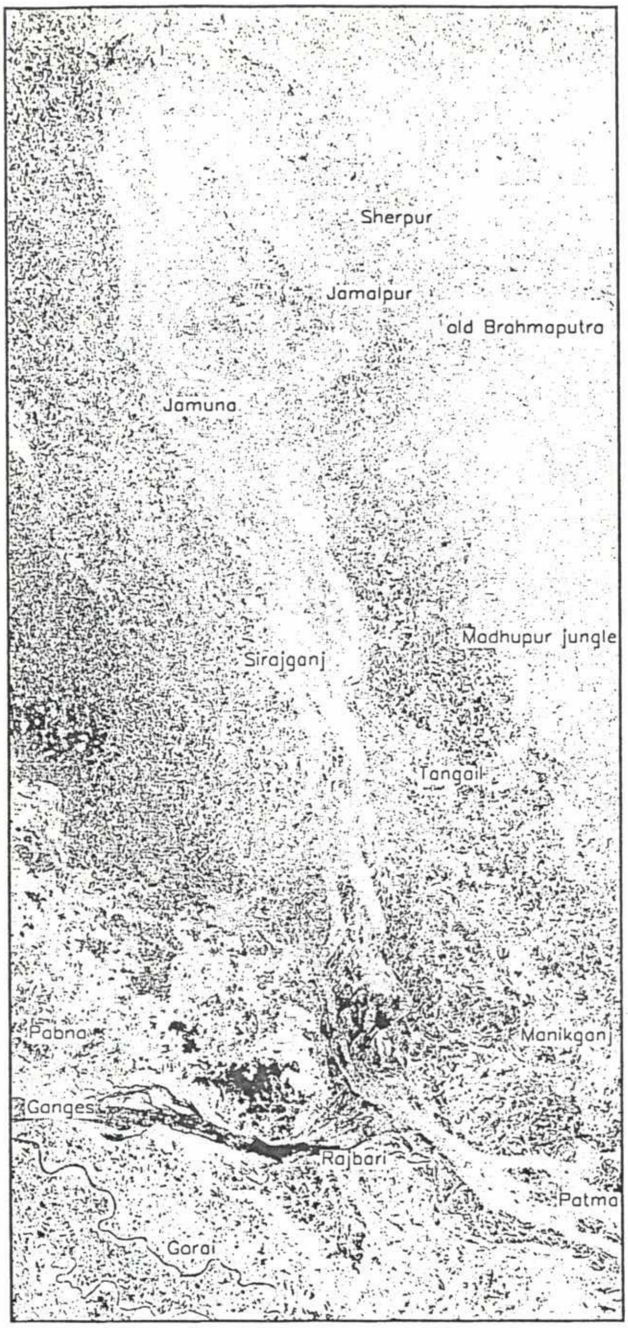

Figure 2 ERS-1 SAR imagery of Bangladesh recorded July 24, 1993. The data range is 8 db. The imagery is presented on a linear grey scale. Image resolution is 100 m x 100 m.

4 Results

In this section several interesting features visible in the SAR imagery will be shown. Due to the wide range of phenomena this presentation may resemble an enumeration of unrelated subjects. Subjects presented in this section are:

- image processing and image enhancement
- infrastructure
  - embankment
  - roads
  - power lines
- soil moisture
- flooded areas
- shallow areas in the Jamuna river
- turbulence

4.1 Image processing

The SAR image shown in Figure 2 lacks contrast in the upper part of the image. This can be improved by adapting the grey scale of the imagery. It is common practice to use, for example, linear stretching or histogram equalization. In Figure 3 the result of moderate histogram equalization is shown. In this figure details at the surface of the river are enhanced and some details on the land are lost.

Figure 3 Histogram equalized imagery of Bangladesh

88

4.2 Infra-structure

Figures 2 and 3 display the position of cities and the main rivers. Cities show up as bright spots. Rivers can be detected by looking for either dark places (no turbulence) or for brighter areas with a characteristic flow pattern. Some smaller details can be detected as well by enlarging specific parts of the imagery. As an example the neighbourhood of the city Sirajganj is shown in Figure 4. Visible are the embankment south of the city, and the groyne in the North. Furthermore, the city-plan, roads and cross-roads can be seen.

Figure 4 Neighbourhood of Sirajganj on the bank of the Jamuna river. Image resolution is 12.5 m x 12.5 m

Not only roads and houses can be observed in the sar images, but also power lines. These lines and their pylons are visible because metal objects reflect the radar signal very well. Figure 5 shows the crossing of such a power line over the Jamuna River. The pylons are about 1200 m apart.

Figure 5 Crossing of a power line over the Jamuna River

4.3 Embankment

Further to the North a retreated embankment can be seen along the Jamuna river (see Figure 6). The embankment has been breached in the past and a new embankment has been built more to the West.

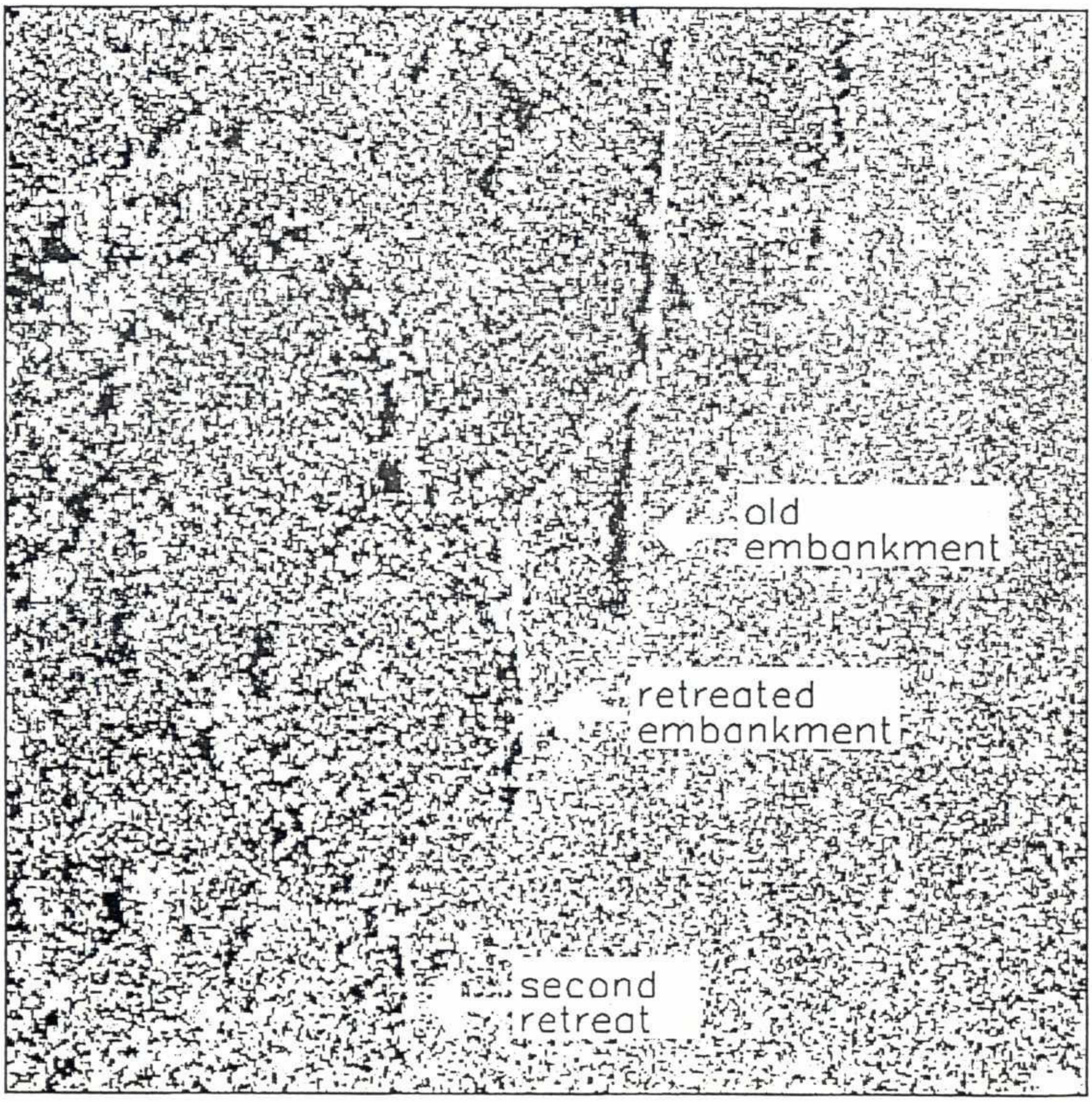

Figure 6 Retreated embankment along the Jamuna river

4.4 Land-water segmentation: flooding

Water and land have a different signature on SAR images. Inspection of the images (see Figures 2 and 3) shows that radar backscatter by still-water surfaces is much lower than radar backscatter by the land surface. However, at some spots radar backscatter by the water surface is higher, probably due to turbulence. Furthermore, the radar backscatter fluctuations as observed over the river, are lower than those observed above the land. The latter is visible in Figure 7. Figure 7 shows the local variation in radar backscatter within squares of 100 x 100 m^2. By setting a fixed threshold and applying a region growing algorithm, all points with a low local variability are connected in Figure 8. Figure 8 shows that all rivers are detected. Furthermore, a region in the mid-left part of the figure is identified as water. According to land-use maps of the area, this region is characterized by: deep water aman (rice) cultivation, and seasonally flooded grazing land. So it is likely that this area is flooded indeed. For comparison a classified SPOT image of 1989 is shown in Figure 9 (from: Bank protection and river training pilot project 1992). Figures 8 and 9 show an intricate networks of flooded areas.

89

Figure 7 Variation in radar backscatter. Resolution 100 x 100 m^2

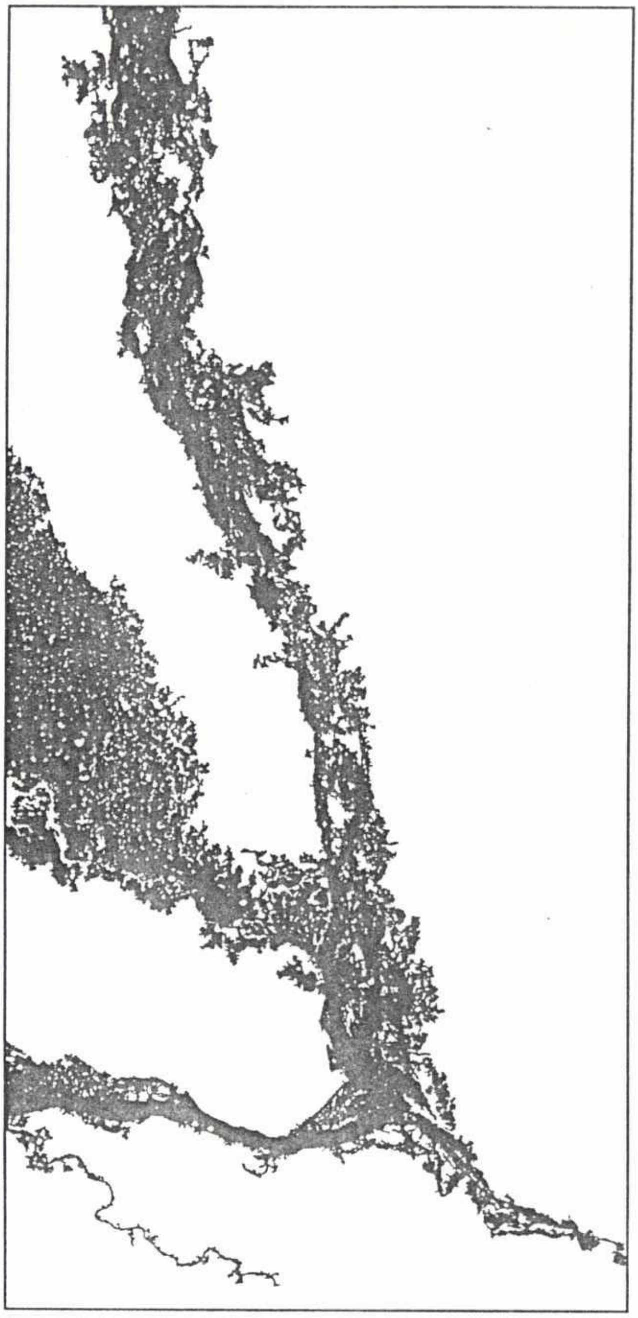

Figure 8 Rivers and flooded areas

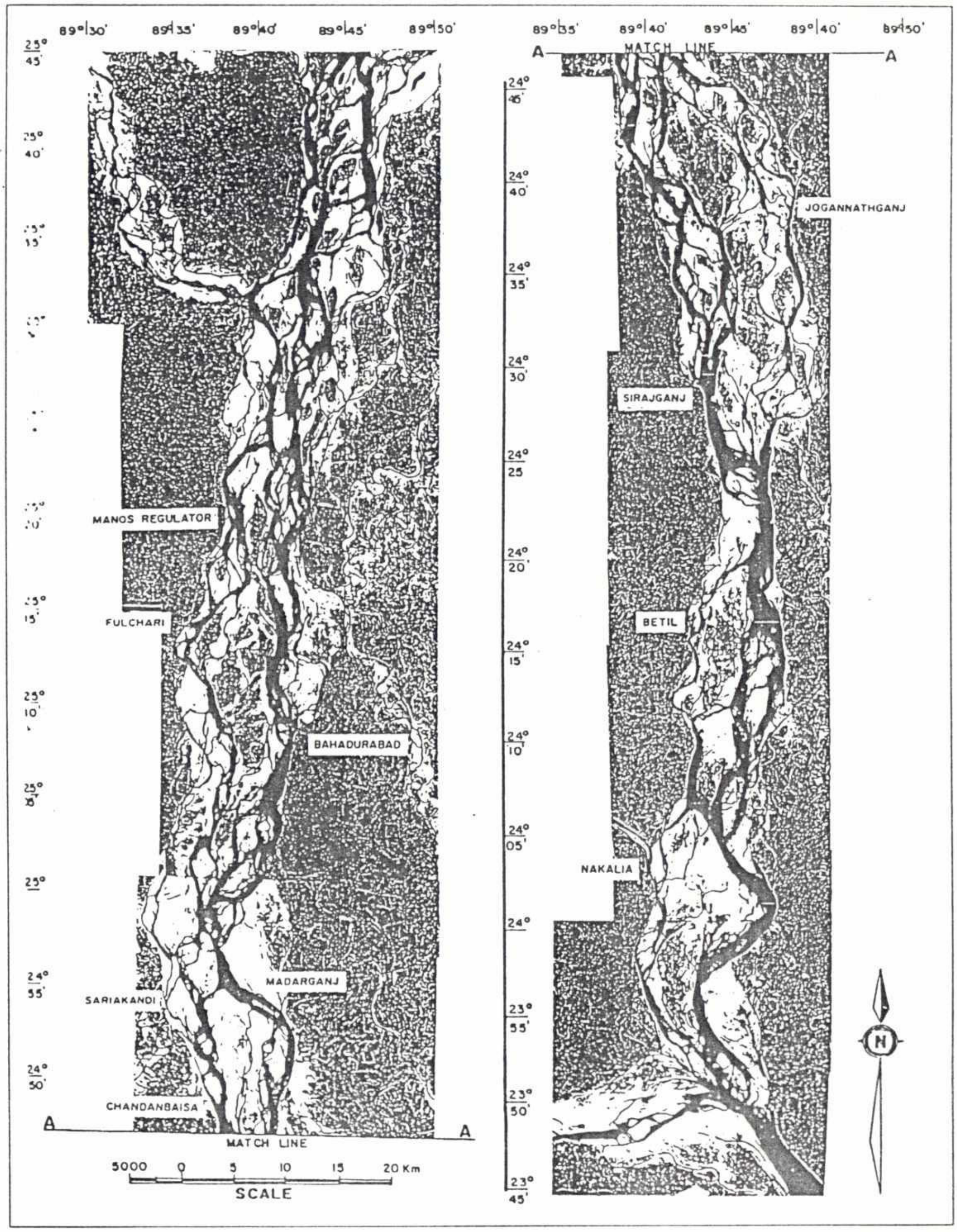

Figure 9 Classified SPOT image, March 1989

80

4.5 Soil moisture

Using SAR imagery it is possible to separate land and water masses. In a more subtle way it is also possible to determine soil moisture. An example is shown in Figure 10. Figure 10 shows the Brahmaputra Right Embankment near the confluence of the Jamuna river and the Ganges. The west side of the embankment is relatively dark. Because radar is more absorbed by wet soil than by dry soil, it can be argued that west of the embankment the soil is dry whereas soil on the riverside it is wet.

Figure 10 Differences in soil moisture

4.6 Bottom topography

In the Jamuna river, close to the confluence with the Ganges, a shallow region can be observed (see Figure 11). This area is visible as a dark spot in the imagery.

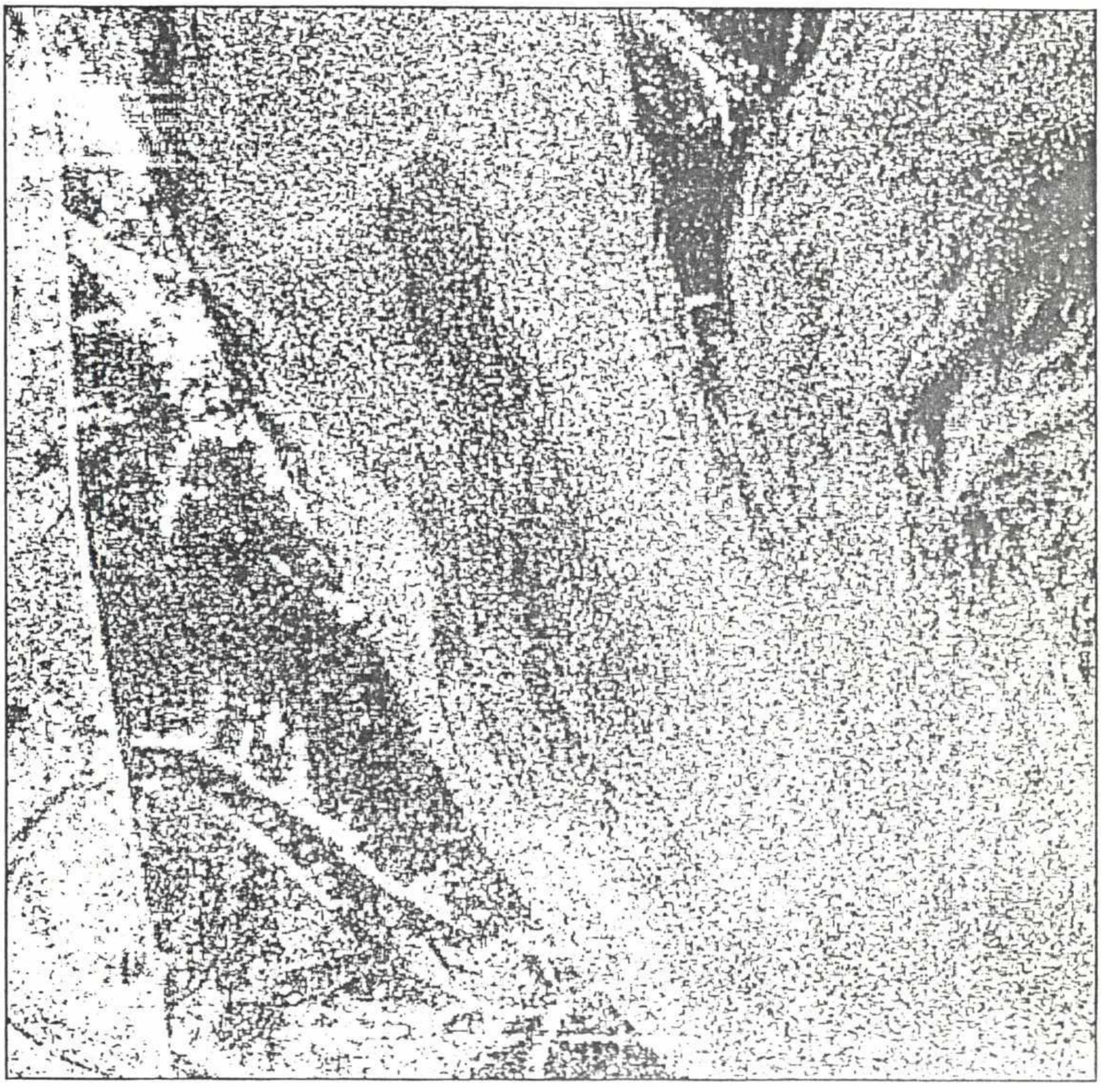

Figure 11 Shallow area in the Jamuna river

Of another area more to the North near Bahadurabad Ghat sounding data were obtained within the framework of the FAP 24 project. These data were interpolated to a depth map. The same area was selected from the ERS-1 SAR images. The SAR data and the depth map are compared in Figure 12. In Figure 12 a clear correspondence is seen between both data sets. Low radar backscatter values correspond to shallow areas and high radar backscatter values correspond to deep areas.

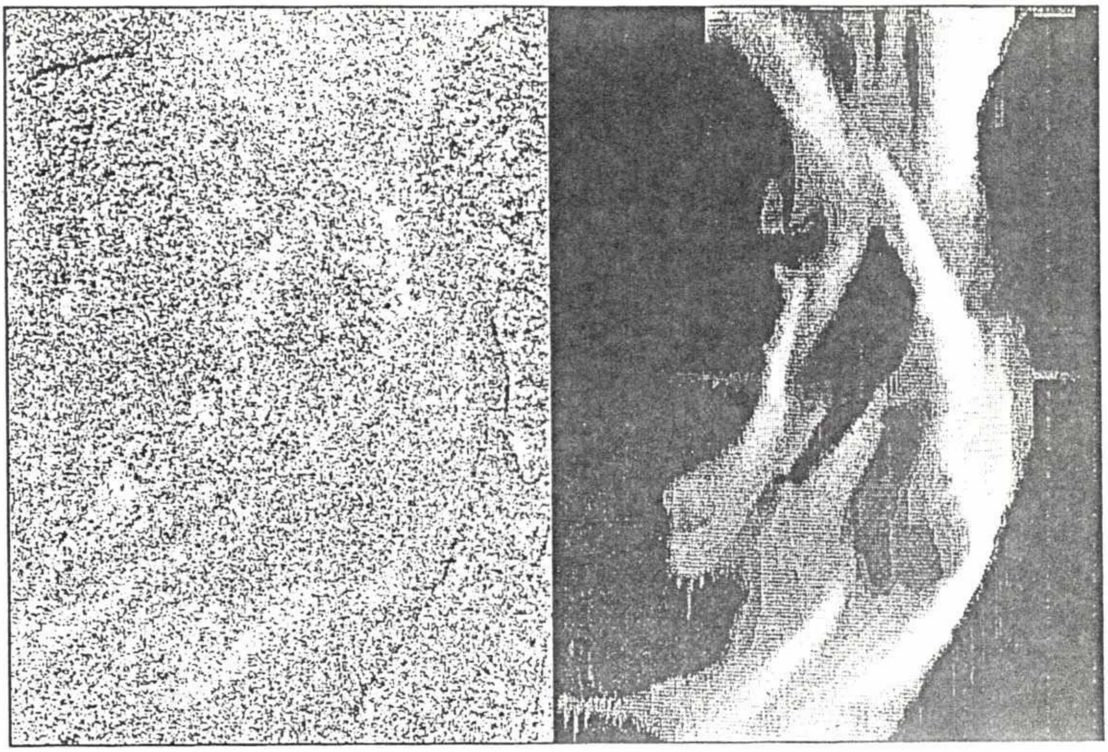

Figure 12 Radar backscatter (left) and depth map (right) of the same area. The depth map is linearly scaled between 0 m (black) and 19 m (white).

4.7 Turbidity

Near the confluence of the Jamuna river and the Ganges there is a char which splits the Jamuna river in two. Downstream of this char the two flows do not merge immediately but coexist for another 5 or 10 km. The two flows are split by a narrow turbid strip of water. This strip is visible as a dark line in Figure 13. Similar features have been observed below confluences in the Zaïre river (Peters, 1993).

Figure 13 Turbid strip in the Jamuna river, area is 12.8 x 12.8 km^2.

4.8 Turbulence

Where the Jamuna river and the Ganges merge the flow velocity of the river increases. This is observed in Figure 14. Due to the high flow velocity the water is very turbulent, which results in a white area in the imagery. The ferry is known to suffer great problems when sailing against the current in the white areas near the bank of Aricha.

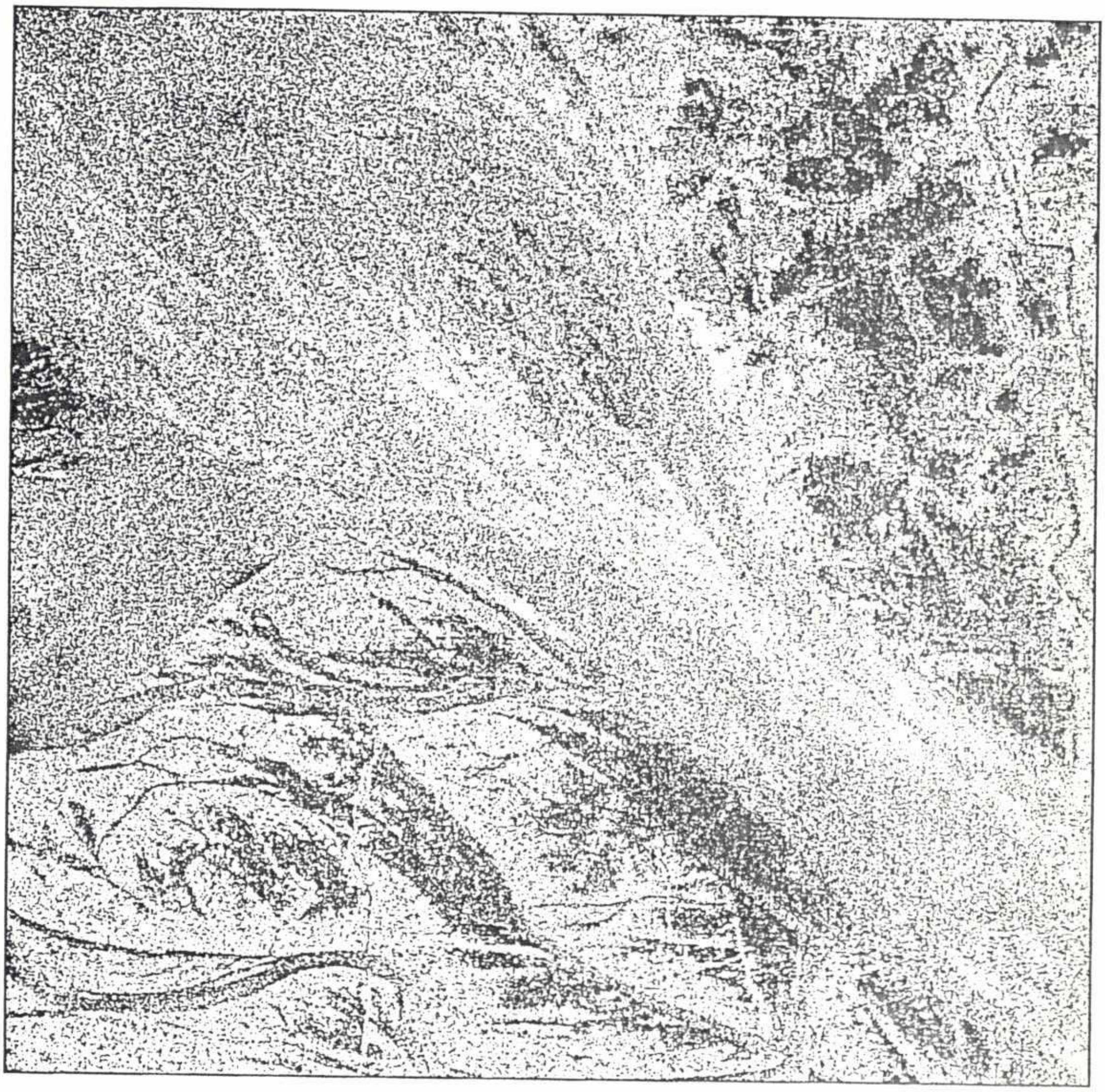

Figure 14 Part of Jamuna river with high flow velocity. Area is 12.8 x 12.8 km^2

4.9 Manos Regulator

The imagery was recorded only one day after the Manos Regulator collapsed into the river as a result of massive bank retreat. The sequence of bank lines is shown in Figure 15, where bank line number 14 corresponds with the bank line at the time of image recording. A few days before, on July 20, the embankment near the Manos Regulator was breached. The water level above the land was then 0.30 m higher than in the Brahmaputra River and the outflowing water reached high flow velocities (Ahmad et al, 1993). The breach and the inundated land behind it are visible in the radar image.

Figure 15 Part of ERS-1 image near the Manos Regulator indicated by the arrow. The area is 15 x 15 km^2

5 Discussion and conclusions

It has been shown that information required by the Bangladeshian authorities can be obtained from radar imagery. The following features were extracted from the SAR data:

- location of infra structure: embankment, roads, houses, power lines, etc,
- position of rivers and flooded areas,
- areas with a different soil moisture,
- bottom topography in the Jamuna river,
- turbidity, and
- turbulence.

The land-water segmentation led to a map of 100 x 200 km^2 showing flooded areas at the time of image recording. The imagery was recorded in the wet season. In this season optical remote sensing is not suitable because of the high levels of cloud cover. The same holds for most of the dry season. The recording of SAR imagery is not affected by cloud cover. Being able to monitor the river embankment at regular intervals is very important. Currently this is not feasible. Field surveys along the whole length of the river just take too much time. ERS-1 images showing the embankment can be obtained at least one or twice every month.

The position of the river bank can be determined and shallow areas can be identified. In a meandering river one usually finds high flow velocities in deep areas and low flow velocities in shallow areas. In general, higher flow velocities result in increased surface roughness. Therefore, shallow areas will be visible as dark spots in the radar image and deep areas will be bright. A quantitative relation between depth and brightness still has to be determined.

The above correspondence between depth and radar backscatter seems not to be valid in part of the Ganges. Part of this river turns out black in the radar image whilst, as far as we know, the river is not shallow in this area. The low radar backscatter indicates that the water surface is rather smooth and that flow velocities are low. This may occur in deep and wide rivers. If this is the case, we do not know.

References

Ahmad, M.U. ,A.K.M.S. Haque, M. Islam, and S.A. Yasuf, *Study report on finding out detailed causes and possible remedy of erosion of the Brahmaputra River on areas adjacent to the Manos Regulator*. Rep. Study Committee, August 1993.

Alpers, W., and Hennings, I., A Theory of the Imaging of Underwater Bottom Topography by Real and Synthetic Aperture Radar, *Journal of Geophysical Research*, Vol. 89, No. C6, pp 10,529-10,546, November, 1984.

Bank protection and river training (AFPM) pilot project FAP 21/22, Technical report no.1, pre-selection of test areas, March 1992, DELFT HYDRAULICS report IQ1326I.

Bank protection and river training (AFPM) pilot project FAP 21/22, Morphological predictions for test areas, November 1993, DELFT HYDRAULICS report IQ1326V.

Calkoen, C.J., Kooi, M.W.A. van der, Hesselmans, G.H.F.M., and Wensink, G.J., *The imaging of sea bottom topography with polarimetric P-, L-, and C-band SAR*. Report BCRS project 2.1/AO-02. Netherlands Remote Sensing Board, Delft 1993.

The Flood Action Plan, Bangladesh, (In Dutch: The Flood Action Plan, Bangladesh, Een onderzoek naar aanleiding van het debat over waterbeheersing in Bangladesh), Inspectie Ontwikkelingssamenwerking te Velde, June 1993.

Klaassen, G.J., Mosselman, E., and Brühl, H., On the prediction of planform changes in braided sand-bed rivers, In: *Advances in Hydro-Science and -Engineering*, Volume I, pp 134-146, Wang S.S.Y. (ed.), 1993.

Peters, J.J. Personal communication, 1993.

Vogelzang, J., Wensink, G.J., de Loor, G.P., Peters, H.C. Pouwels, H., and van Gein, W.A., *Sea bottom topography with X-band SLAR*, BCRS report, BCRS-89-25, 1989.

• location 'De Voorst'

• main office

main office
Rotterdamseweg 185
p.o. box 177
2600 MH Delft
The Netherlands
telephone (31) 15 - 56 93 53
telefax (31) 15 - 61 96 74
telex 38176 hydel-nl

location 'De Voorst'
Voorsterweg 28, Marknesse
p.o. box 152
8300 AD Emmeloord
The Netherlands
telephone (31) 5274 - 29 22
telefax (31) 5274 - 35 73
telex 42290 hylvo-nl

North Sea

• Amsterdam

• London

Brussels •

TV

Appendix C

Application of ERS-1 SAR data to support the routing of offshore pipelines

Reprint of DELFT HYDRAULICS report H1787
by
G.H.F.H.Hesselmans, G.J.Wensink, C.J.Calkoen & H.Sidhu (1994).

Executive's summary

Knowledge of the sea bottom topography is essential for activities such as shipping, fishing, dredging, offshore construction and pipeline laying, amongst other things. Assessment of the sea bottom topography with present state-of-the-art techniques (ship-based echosounders) may become relatively expensive and it is expected that a combination of traditional methods with remote sensing (RS) techniques may greatly reduce survey costs.

Methods of obtaining bathymetric information from remote sensing (RS) imagery have been developed at DELFT HYDRAULICS, with support from the Netherlands Remote Sensing Board (BCRS) and the European Community (EC). A great step forward has recently been taken in this field by the development of a so-called Bathymetry Assessment System which combines echosounding and Synthetic Aperture Radar (SAR) observations.

These RS-based methods are now ready for introduction to commercial operations. An ideal way to show them would be to carry out demonstration projects. The purpose of the demonstration project presented within this report is to show that the combined use of ERS-1 (First European Remote Sensing Satellite) SAR and *in-situ* observations is more cost effective than only traditional bathymetric surveys.

This demonstration project has been carried out in close connection with OCEONICS INTERSITE B.V., utilising information acquired during the ZEEPIPE DEVELOPMENT project (1991–1992). The ZEEPIPE DEVELOPMENT included the laying of several pipelines from a Norwegian gas field, including one to the Belgian town of Zeebrugge. Part of this project included the execution of detailed multibeam bathymetric surveys by OCEONICS INTERSITE in the southern North Sea to investigate sandwave activity and excavation effectivity. The bottom topography of the area in question is characterized by numerous sand waves and bars which together with the strong regional tidal currents provide ideal conditions for the application of SAR imagery for bathymetric purposes.

Bathymetric information is vital for the safe and proper routing of offshore pipelines. In general, offshore pipeline projects include five stages within which surveys are executed:

- reconnaissance survey,
- route survey,
- pre-lay survey,
- as-laid survey,
- as-built survey.

The techniques presented in this report allow future users to design possible routes prior to the performance of the reconnaissance, route and pre-lay surveys.

For the reconnaissance phase, estimates of the sea bottom topography across large areas are required to select the most promising route. Usually, these estimates are based on existing data which may or may not be up-to-date. For the reconnaissance phase, a survey is generally performed along the most promising route. During the route survey phase, additional tracks are being investigated at offsets of a few hundred metres from the proposed route so as to verify the pipelay corridor and to optimize the pipeline track. In the pre-lay

survey the selected track is surveyed generally ahead of the lay vessel to once again verify the lay corridor and possibly to assess any required dredging effort.

In this reconnaissance study, SAR imagery and existing depth information from Admiralty Charts were used to provide depth estimates of an area covering about 50 km by 50 km. Also investigated was the suitability of SAR data in order to reduce survey efforts in later stages, either by extrapolation of a single line survey and/or for smart interpolation between additional survey tracks.

It has been demonstrated that in the reconnaissance phase SAR data is a valuable information source that can be used for rapid updating of bathymetric charts or confirmation that the information in the chart is right at relatively low cost. Depth accuracy is of the order of a 100 cm and the delivery time is of the order of 3 weeks, assuming that the SAR data have been archived at ESA. Costs are also greatly reduced (often by a factor of 5 to 10) when compared to traditional echosounding.

As for the route survey phase it has been demonstrated that the combination of echosounding data and SAR observations can be used to improve the accuracy of the SAR-based bathymetric map and to reduce survey efforts. For example, based on data from a single line survey, a regional depth map can be constructed with an accuracy of the order of 40 cm.

It is concluded that currently the use of ERS-1 SAR imagery is effective both for the reconnaissance and route survey phases. Depending on the required accuracy, survey efforts at later stages can be reduced considerably when combining echosounding and SAR data with the help of the Bathymetry Assessment System. For example, if a depth accuracy of 30 cm is required with a spatial resolution of 30 m along a 200 m wide corridor, only two echosounder tracks will be required to accurately assess depths along this strip. Consequently, survey costs may be reduced by a factor of up to ten, depending on the scope of the work.

Contents

1 Introduction

Knowledge of the sea bottom topography is essential for activities such as shipping, fishing, dredging, offshore construction and pipeline laying, amongst others' things. Assessment of the sea bottom topography with present state-of-the-art techniques (ship-based echosounders) may become relatively expensive and it is expected that a combination of traditional with remote sensing (RS) techniques may greatly reduce survey costs.

Methods of obtaining bathymetric information from remote sensing imagery (RS) have been developed at DELFT HYDRAULICS, with support from the Netherlands Remote Sensing Board (BCRS) and the European Community EC. These RS-based methods are ready now for introduction to commercial operations. An ideal way to show them would be to carry out demonstration projects. The purpose of the demonstration project presented within this report is to show that the combined use of ERS-1 SAR (First European Remote Sensing Satellite, Synthetic Aperture Radar) and *in-situ* observations is more cost effective than only traditional bathymetric surveys.

This demonstration project has been carried out in close connection with OCEONICS INTERSITE B.V., utilising information acquired during the ZEEPIPE DEVELOPMENT project (1991-1992). The ZEEPIPE DEVELOPMENT included the laying of several pipelines from a Norwegian gas field, including one to the Belgian town of Zeebrugge (see Figure 1). Part of this project included the execution of detailed multibeam bathymetric surveys by OCEONICS INTERSITE in the southern North Sea to investigate sandwave activity and excavation effectivity.

The project area is limited to a section of 32 km length, commencing at Zeebrugge harbour and proceeding seawards. The bottom topography of the area is characterized by numerous sand waves and bars which together with the strong regional tidal currents provide ideal conditions for the application of SAR imagery for bathymetric purposes. Prior to using the ZEEPIPE data for this demonstration project, formal permission had been requested and obtained from NORSKE STATS OLJESELSKAP (STATOIL).

Depth information is required during several stages of any pipeline development, such as the ZEEPIPE project. The required depth accuracy depends on the stage of the project and, in general, five survey stages may be identified:

1) Reconnaissance Survey
   Based on existing data such as Admiralty Charts, the most promising track is selected and surveyed. The aim of this survey is to detect uncharted obstacles such as cables, ship wreckage, sand waves and so on.

2) Route Survey
   Additional lines will now be surveyed at offsets up to a few hundred metres at either side of the proposed route. The aim of this survey is to optimize the pipeline track and to verify the piperoute corridor. Selection of the tracks may be based either on existing data or on the newly acquired survey results. However, both data sets are generally not integrated.

3) Pre-lay Survey
Based on the previous surveys the final pipe route corridor is confirmed and the data may also be used to assess any possible dredging effort. The width of the surveyed strip is generally a 1000 m and the required depth accuracy is about 20 cm.

4) As-laid Survey
After pipelay, a single line survey is being executed to confirm that the pipeline has been laid within the design criteria. This survey can also form the basis of a pre-dredge survey.

5) As-built Survey
The final survey on completion of all construction works.

Bathymetric information from RS imagery is complementary to the information obtained with traditional echosounders. The latter gives highly accurate depth measurements at a point or along a line whereas RS data yield a synoptic two-dimensional overview but usually not with the same overall accuracy.

A great step forward has recently been taken in this field by the development of a so- called Bathymetry Assessment System, combining echosounding and ERS-1 SAR-observations in the following way:

i. based on SAR imagery a first guess of depth is made by analytical inversion of a relatively simple imaging model;
ii. the first guess of depth is used to plan detailed traditional surveys;
iii. final depths are constructed from radar imagery by numerical inversion (data-assimilation) of the imaging mechanism using the traditional observations as constraints.

The techniques presented in this report allow the users to design possible routes prior to the performance of the reconnaissance, route and pre-lay surveys.

In Chapters 2 and 3 of this report the problem is defined and methods to solve the problem are presented. In Chapter 4 the Bathymetry Assessment System is described. Chapter 5 shows the remote sensing data, sounding data and Admiralty Chart data. The results are presented in Chapter 6. Finally in Chapter 7 the results are discussed and in Chapter 8 the conclusions are presented.

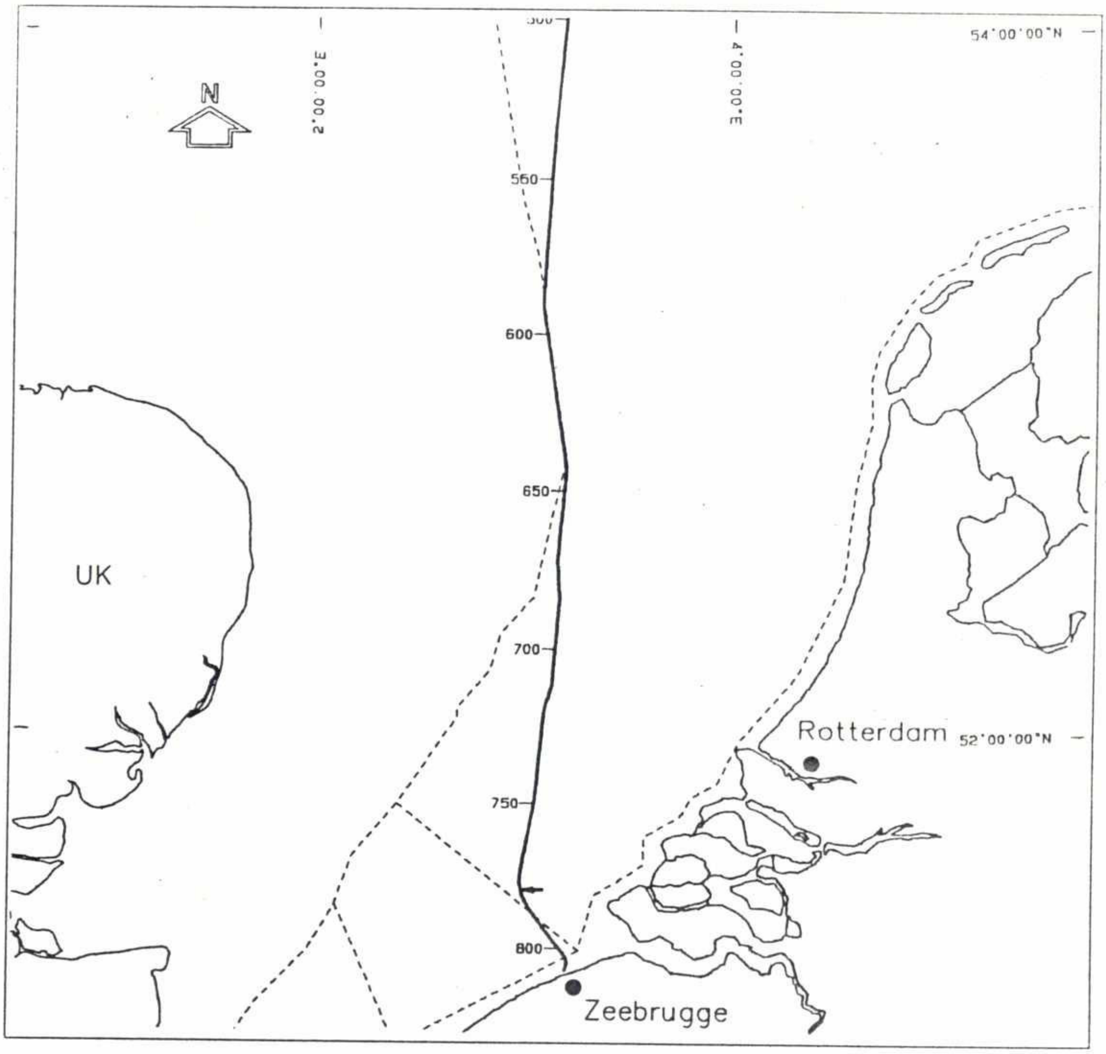

Figure 1 Project site

2 Problem definition

Presently, accurate depth information for pipeline laying is obtained by ship-based (single point or multibeam) echosounders. ERS-1 SAR data yield new opportunities to obtaining depth information.

The information requirements and specifically the accuracy of bathymetry depends on the project stage. In view of the accuracy achievable by ERS-1 SAR-based techniques, this study will focus on the support of the first three survey phases (reconnaissance, route, pre-lay).

Prior to the *reconnaissance survey*, existing depth information, usually derived from Admiralty charts, is combined with ERS-1 SAR data. Prior to the *route survey*, the data from the reconnaissance survey are added to improve the depth map. Prior to the *pre-lay survey* the multi-track route survey data are finally integrated with the ERS-1 SAR data to obtain final depth estimates. The problem addressed in this report is how to use to ERS-1 SAR most efficiently, given the other data and how to produce the best depth maps.

3 Method

Survey efforts during a pipeline project may be reduced by using the most recent depth maps and existing depth information can be updated by using ERS-1 SAR data.

In order to assess the influence of ERS-1 data, depth maps were produced for the first three phases of the ZEEPIPE pipeline project. These maps were created using the Bathymetry Assessment System, combining SAR imagery and traditional depth information (Admiralty chart data and multibeam echosoundings) as would have been available at the date of the phase under consideration. Any additional sounding data were used to further verify the depth estimates.

The quality of the depth maps was quantified by the average prediction error, the root mean square difference and the average absolute difference, denoted "bias", "rms" and "abs" respectively. Measurements obtained during each phase of the project were reconstructed by digitizing a contour map resulting from the pre-lay survey. In the remainder of this section the three methods will be described in relation to the survey.

Reconnaissance Survey

Traditional depth information available prior to this survey stage consisted of an Admiralty chart which was digitized. In addition, ERS-1 SAR imagery was transformed into depth information by means of the Bathymetry Assessment System, described in more detail in Section 4. The Admiralty Chart data were used as boundary conditions by the Bathymetry Assessment System and the end result was the so-called pre-reconnaissance map.

The SAR data provided the small-scale depth changes whereas the Admiralty data yielded the average depth and depth modulations. The latter were assumed to change only slightly in time and so, in a sense, the SAR data were used either to confirm the existing data or to update them. The result was evaluated by comparing the depth estimate with the acquired sounding data along the pipeline track.

Route Survey

Prior to the route survey, the single track reconnaissance survey became available and was also included in the boundary conditions of the Bathymetry Assessment System. The resulting depth map was the so-called pre-route map. In a sense the survey data were extrapolated perpendicular to the track, the result was evaluated by comparing the depth estimates with existing multibeam sounding data at a 100 m offset from the central track.

Pre-lay Survey

The distance between section lines measured during the route survey exceeded the beamwidth of the multibeam echosounder used during the traditional surveys. Therefore interpolation techniques were required to estimate depths between the sailed lines. This interpolation was achieved by including the route survey data in the boundary conditions of the Bathymetry Assessment System, digitized from the boundary of the sounded area. The quality of the interpolation was assessed by comparing results with measurements along the central track.

In addition, the impact of the ERS-1 SAR data was assessed by comparing results with estimates obtained by linear interpolation.

4 Bathymetry Assessment System

Under favourable meteorological and hydrodynamic conditions (moderate winds and strong tidal currents), air- and space borne Synthetic Aperture Radar (SAR) imagery shows features of the bottom topography of shallow seas (Alpers and Hennings 1984, Vogelzang et al., 1989).

It is generally accepted that the imaging mechanism consists of three stages (a more detailed mathematical formulation is given in Calkoen et al., 1993):

(1) Interaction between (tidal) flow and bottom topography results in modulations in the (surface) flow velocity. This relation can be described by several models with an increasing level of complexity: continuity equation, shallow water equations, and the Navier Stokes equations.

(2) Modulations in surface flow velocity cause variations in the surface wave spectrum. This is modelled with the help of the action balance equation, using a relaxation source term to simulate the restoring forces of wind input and wave breaking.

(3) Variations in the surface wave spectrum cause modulations in the level of radar backscatter. To compute the backscatter variations a simple Bragg model can be used, but also available are two-scale and first iteration Kirchoff (Holliday) models.

Based on the above three stage mechanisms, a train of computer models has been developed at DELFT HYDRAULICS. Models with different levels of complexity and physical detail are available for each step. These models describe the flows, waves and electromagnetic scattering and can be used to interpret radar images.

The above package makes it possible to determine the radar backscatter given the depth. In order to invert this depth-radar backscatter relation, a data assimilation scheme has been developed, minimizing the difference between the predicted and the measured radar backscatter by adapting the bottom topography.

The structure of this modular system is shown in Figure 2.

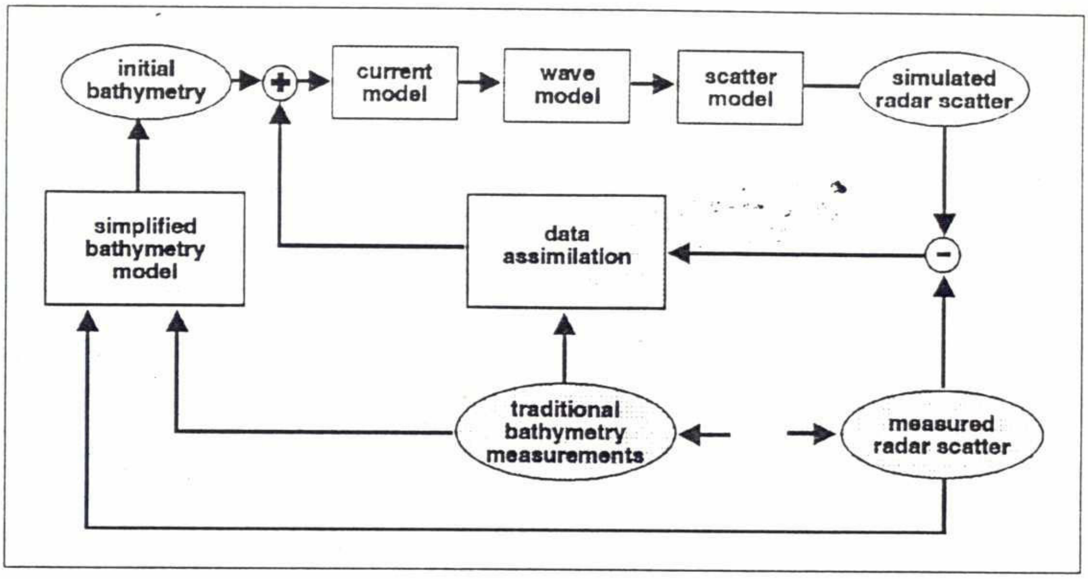

Figure 2 Bathymetry Assessment System

Implementation

In the previous section a mechanism relating depth to the radar backscatter has been introduced. Based on this mechanism a modular imaging model has been implemented at which each module corresponds with a step in the imaging mechanism:

- flow model,
- short wave spectral model, and
- radar backscatter model.

As previously stated, these models can be made with different levels of complexity. For example in shallow coastal areas with complex bottom topography a two- or even three-dimensional flow model may be needed to assess the surface flow. However, in general such sophisticated models are not required and simpler models can also be used. In this paper results are presented of the study at the Belgian landfall of one of the ZEEPIPE lines. The physical processes in this area are described by one-dimensional models and so the description of the Bathymetry Assessment System will be limited to these one-dimensional models. The actual implementation of the system is such that any of these one-dimensional models can easily be substituted by two- or even three-dimensional models, if dictated by the complexity of the area. The following sections describe the modules of the Bathymetry Assessment System:

Flow model

The flow model determines the surface current in two steps. Firstly, the depth-averaged flow is determined by means of the continuity equation. Based on the depth-averaged flow, wind speed and depth the surface flow is calculated by a dynamic flow profile model, allowing for the effects of Coriolis forces and turbulence.

Short wave spectral model

The spectrum (A) for short waves is determined by the action balance equation. This partial differential equation can be reduced to an ordinary differential equation along a characteristic:

$$\frac{dA}{dx} = -R(A - A_0)$$

where the relaxation parameter R depends on wind speed, wave velocity and surface current. For the equilibrium spectrum (A_0) we take the Philips spectrum. The above differential equation can be solved analytically and in order to obtain a solution on a discrete grid, we assume that the relaxation parameter R is constant between two grid points x_n and x_{n+1}. If the relaxation parameter is large, a good estimate of $A(x_{n+1})$ can be found by assuming that the spectrum was in equilibrium in the previous grid points.

Radar backscatter model

The radar backscatter is based on the Bragg mechanism. The radar backscatter is proportional to the wave energy at the Bragg wave number, which is of the same order as the radar wave number. The proportionality constant depends on the incidence angle, radar wave length and polarization. As for the bathymetry system only backscatter variations in the SAR image are relevant, all radar measurements are preprocessed, subtracting empirically-obtained equilibrium values.

Data assimilation

The model train described above simulates the radar backscatter for a given bottom topography. The aim of the data assimilation scheme is to invert this relation and assess a reconstructed bottom topography, given the measured radar backscatter and *in situ* measurements such as soundings. This is achieved in two steps:

1) A first-guess bottom topography is obtained by inversion of a simplified bathymetry model, which is linearized around a best-guess working point. A smoothness condition is imposed in order to reduce the effect of speckle noise.

2) A quadratic cost function is constructed from the difference between the measured and simulated SAR image and the difference between calibration and reconstructed depths. Minimization of this cost function yields the reconstructed bottom topography.

5 Project site and available data

The site northwest of Zeebrugge encompassed a corridor of 32 km x 200 m, the longitudinal axis of which was the actual pipe route. In order to construct the depth maps in this area the following three data sets were used:

- multibeam echosounding data,
- SAR images,
- Admiralty Chart.

Multibeam Echosoundings

The sounding data were provided by OCEONICS INTERSITE for STATOIL in the period between February 19, and March 31, 1992. These data were acquired with a multi-beam echosounder and covered an area of about 200 km x 200 m; kilometre points (KP) were defined in the along track direction. The whole track extended from KP 600 to KP 807 (Zeebrugge). Soundings from the pre-lay survey between KP 775 and KP 807 were used for this demonstration project. In order to cover the 200 m wide corridor, 15 parallel tracks were surveyed by a multibeam sounder and based on these, bathymetric maps were constructed. Figure 3 shows a small section of the corridor, represented as a contour plot.

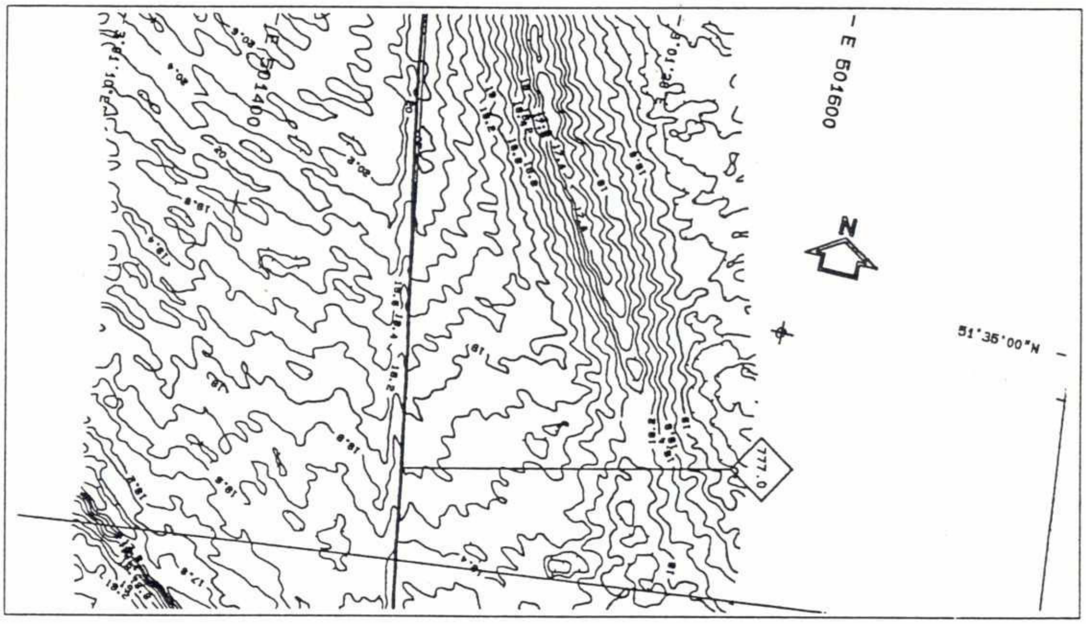

Figure 3 Bottom topography of a small section of the surveyed strip

Spatial coordinates are given for both geographical (latitude, longitude) and UTM coordinates. Within the UTM system the x-coordinate lay between 501250 and 516528, the y-coordinate ranged from 5688920 to 5719897. The depth accuracy was 20 cm and the range of depth values lay between 3.80 m and 38.0 m along the pipe route.

Figure 4 (solid line) shows the bottom profile along the centreline of the 32 km long corridor. Large depth modulations between 10 and 20 m were observed; sand waves with an amplitude of the order of 1 m and a wavelength between a 100 and 200 m were found along the pipeline track.

96

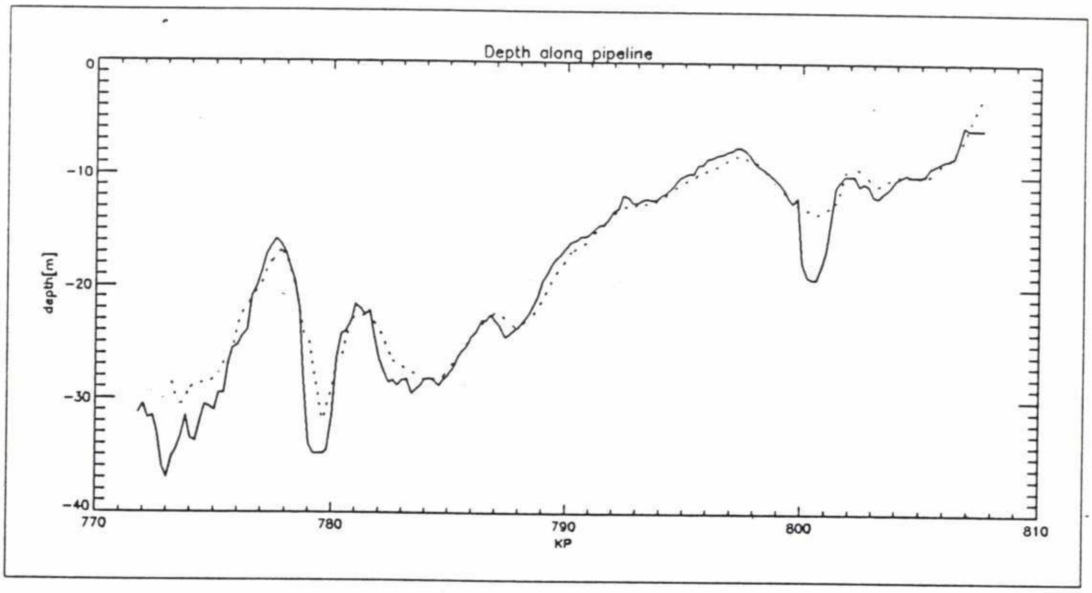

Figure 4 Depth along pipeline track. Solid: sounding data recorded in 1992; Dots: data obtained by digitizing an Admiralty Chart based on soundings in the period 1982-1991

ers-1 sar imagery

Based on current and wind information, two potentially suitable images were selected and ordered from ESA. These image were recorded on April 29, 1992 and September 1, 1993. Relevant sections of these images are shown in Figures 5 and 6. The images had a pixel size of 12.5 m x 12.5 m and 20.0 m x 15.8 m whereas the spatial resolution of both images is about 30 m. The data were projected on the UTM coordinate system WGS-84 (semi major axis 6378137.000 m, semi minor axis 6356752.314 m).

The image recorded on April 29, 1992 did not sufficiently reveal bottom features to allow depth determination whereas the image recorded on September 1, 1993 clearly showed features lying parallel to the coast. This was attributed to the hydro-meteorological conditions at the time of recording of the two SAR images; these conditions are presented in Table 1.

	April 29, 1992	**September 1, 1993**
recording time (GMT)	10:43	10:43
flow velocity	0.4 - 0.8 m/s	0.3 - 0.6 m/s
flow direction	southwest to northeast	northwest to southeast
wind speed	7-8 m/s	2-3 m/s
wind direction	west-north-west	north-north-west

Table 1 Hydro-meteorological conditions at the time of recording of the ERS-1 SAR data

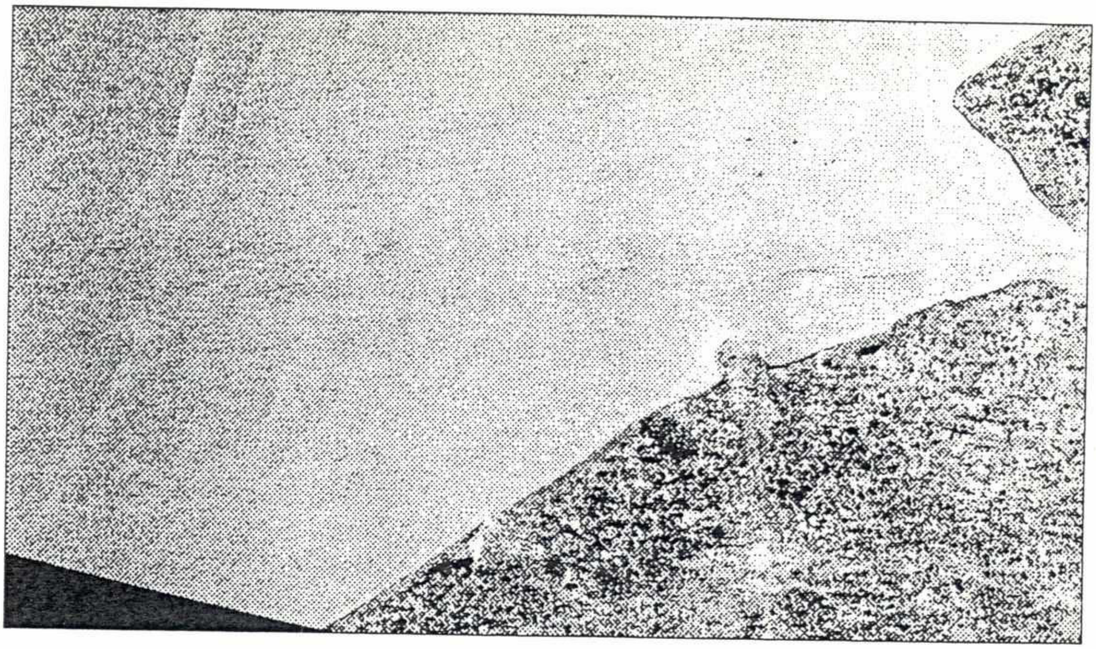

Figure 5 Part of ERS-1 SAR precision image recorded 10:43 April 29, 1992. Area dimensions 84x48 km^2

The image of September 1, 1993 more clearly revealed seafloor structures lying parallel to the shoreline and so the results presented in this report are based on this image (Figure 6); the dark line indicates the pipeline track superimposed onto the SAR imagery.

Admiralty Chart

Admiralty Chart INT 1474, as published by the Netherlands Hydrographer in June 1993, was partly digitized to obtain depth information at offsets greater than a 100 m from the pipeline track. Contour information of the Belgium part of the Admiralty Chart was based on sounding data collected in the period 1982-1991 whereas data of the Dutch waters was based on surveys in the period 1977-1989. The depth data in the Admiralty Chart were reduced to low water spring, whereas the sounding data were reduced to Long Term Mean Sea Level (MSL) and so, the Admiralty data were adapted to MSL. The dotted line in Figure 4 gives the depth along the track of the pipeline: a contour map of the area of interest is presented in Figure 7.

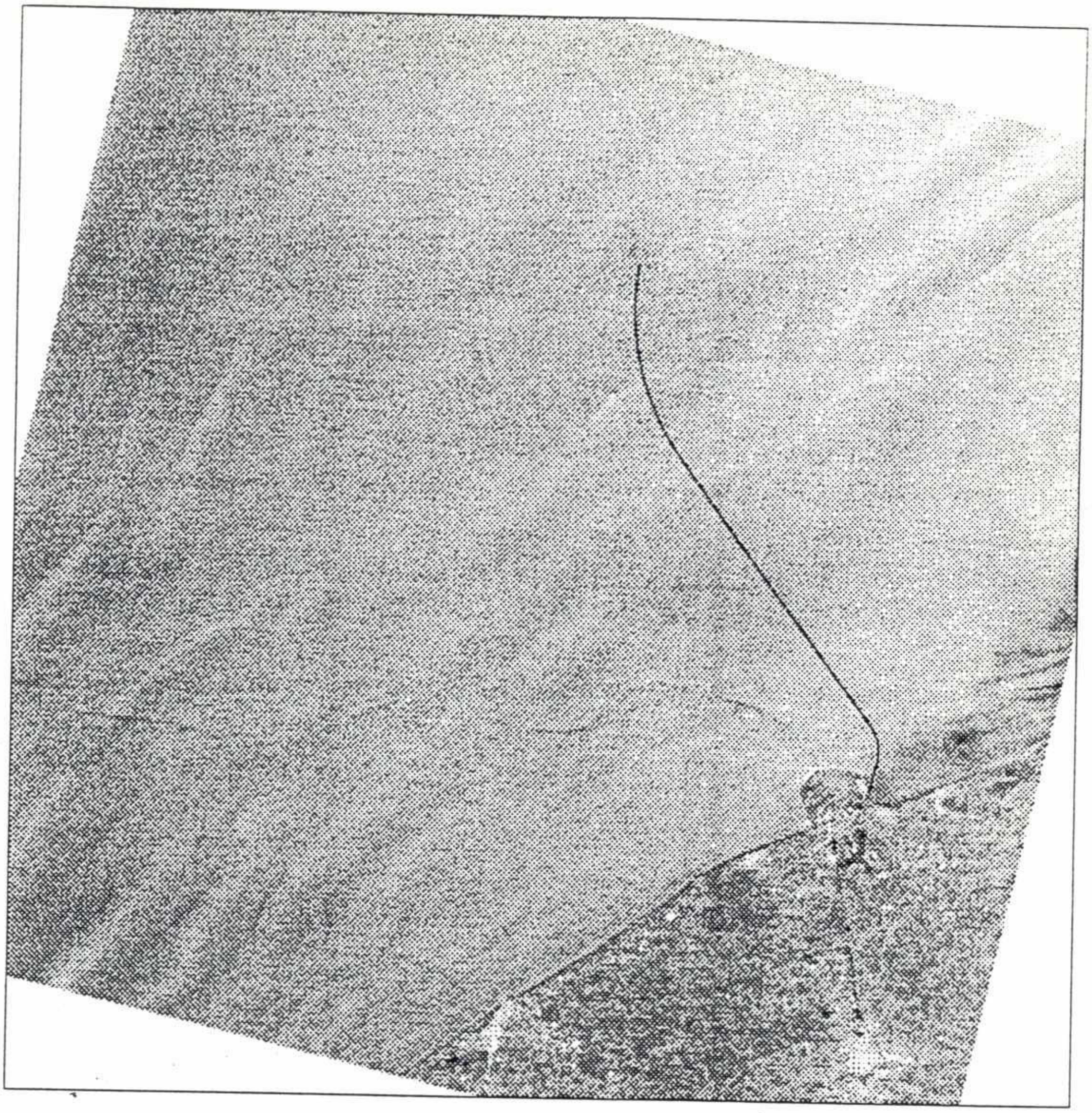

Figure 6 Part of ERS-1 SAR image recorded 10:43 September 1, 1993. Area dimensions 64x64 km^2. The black line indicates the pipeline track

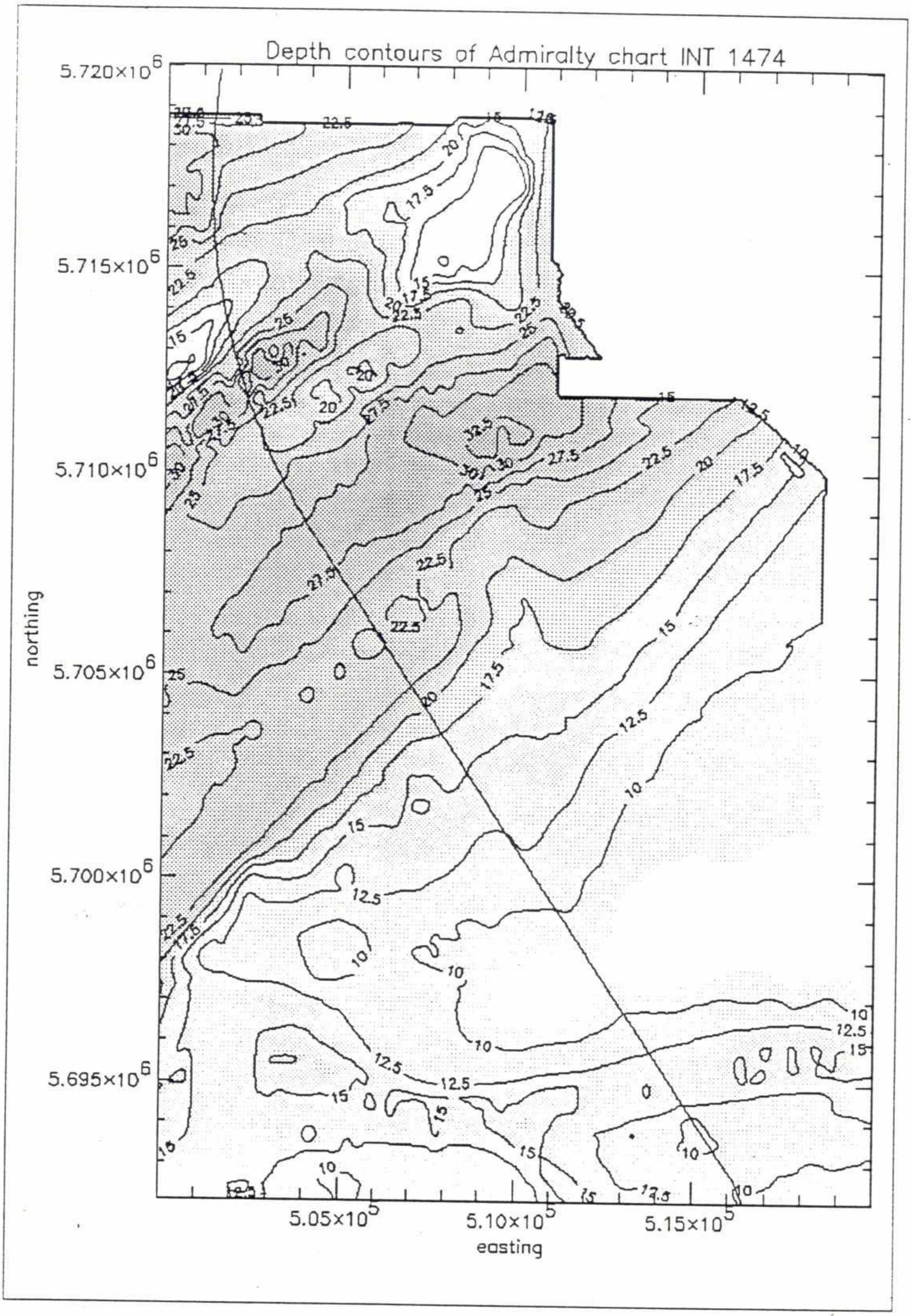

Figure 7 Contour plot of bottom topography based on Admiralty Chart data. Coordinates defined within UTM system. Line segment indicates track of pipeline

Data comparison

The track of the pipeline was shown on Admiralty Chart INT 1474 but comparison of the digitized position of the charted track and the track as determined from the multibeam surveys showed maximum positional errors of approximately a 100 m. This error corresponded to 0.2 mm as measured on the Admiralty Chart.

The differences between the Admiralty Chart and the sounding data were rather large (see Figure 4) and at least two reasons for these differences could be proposed:

1) Temporal difference.
   The Admiralty data were collected in the period 1982-1991 while the pipeline track was surveyed in 1992. The depth of the "Scheur" Channel according to the multibeam sounding and the Admiralty Chart data was found to be 19.2 m and 17.4 m respectively. An even older Admiralty Chart (1442 N) based on surveys in the period 1969-1973 gave an even smaller depth of 13.0 m. Apparently the depth in the channel has increased rapidly with time.

2) Purpose.
   Admiralty Chart data are designed for safe shipping. Therefore, indicated depths tend to be too low and localised details are usually not indicated in these maps.

6 Results

The three maps for the consecutive survey phases are presented in this section.

Reconnaissance Survey

An updated map of the bottom topography was made based on the SAR data and general information about the average depth and trends in the area. The end result, the pre-reconnaissance depth map, is shown in Figure 8; general trend information was obtained from the Admiralty Charts (see previous section). The bottom topography was dominated by large-scale structures lying parallel to the coast line and depth changes of 20 m occurred over distances of some 2 km. No sand waves or sand banks perpendicular to the coast line were found. This pre-reconnaissance depth map was compared with the sounding data along the pipeline track. The same was done with respect to the Admiralty Chart data and the results are presented in Figure 9 and Table 2.

	bias [cm]	rms [cm]	abs [cm]
Admiralty Chart data	75	214	127
Pre-reconnaissance depth map	49	135	90

Table 2 Comparison of soundings, pre-reconnaissance depth map and Admiralty Chart data. "Bias" indicates the average difference between soundings and pre-reconnaissance depth map (or Admiralty Chart data), " rms" indicates the root mean square difference, "abs" the average absolute difference and "max" the maximum absolute difference

Both the pre-reconnaissance depth map and the Admiralty Chart data showed a bias due to the fact that the depth in the channels was underestimated. The other errors were also rather large for the same reason. Note, however, that the errors in the pre-reconnaissance depth map were considerably smaller than those in the Admiralty Chart data in spite of the fact that the bathymetry model had been calibrated using the apparently out-of-date Admiralty Chart data. The maximum error had been reduced by 4.78 m, i.e. from 1122 cm to 644 cm. This improved depth estimate is clearly visible in Figure 9 near KP 800.

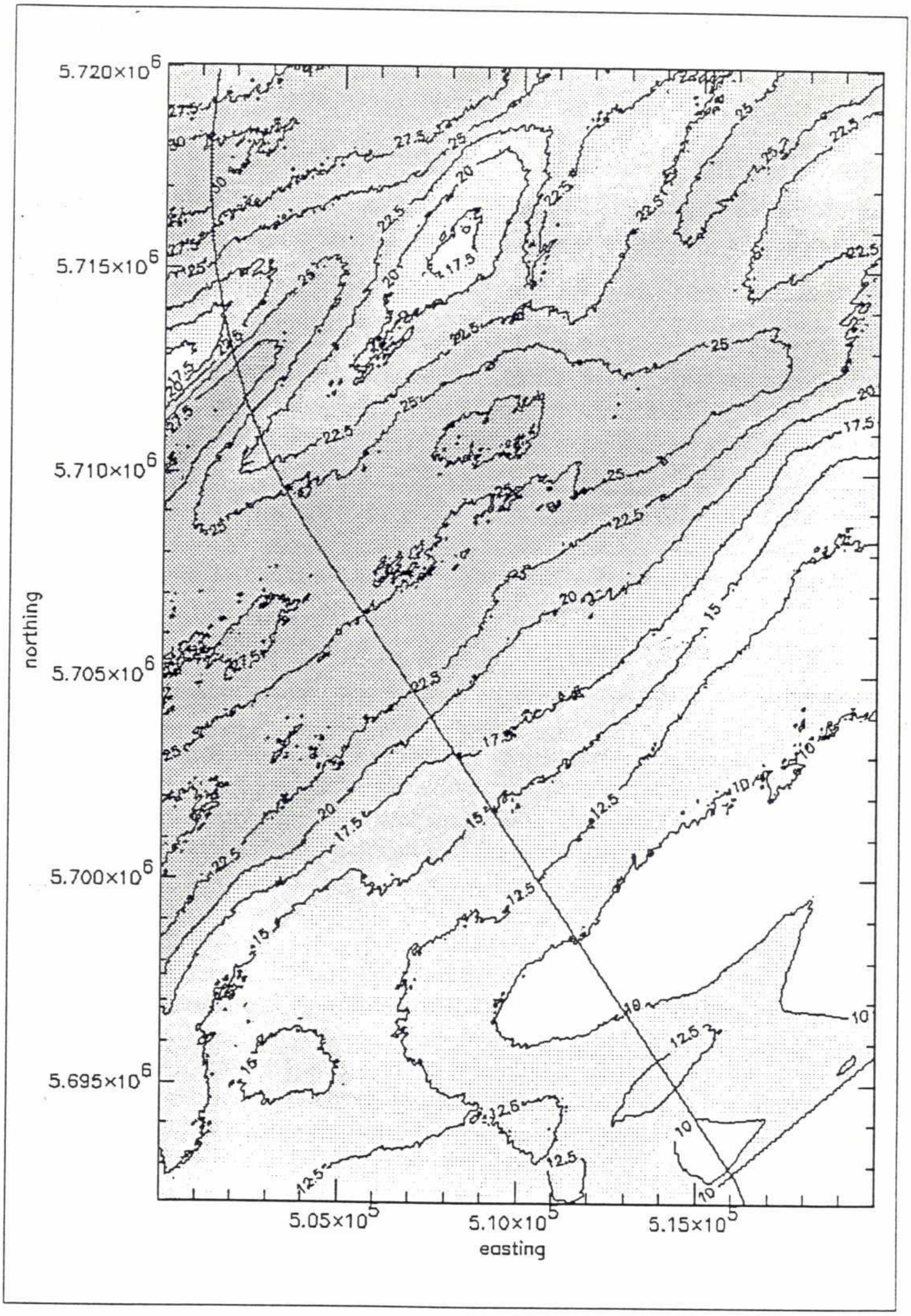

Figure 8 Pre-reconnaissance depth map. Coordinates defined within UTM system. Line segment indicates track of pipeline

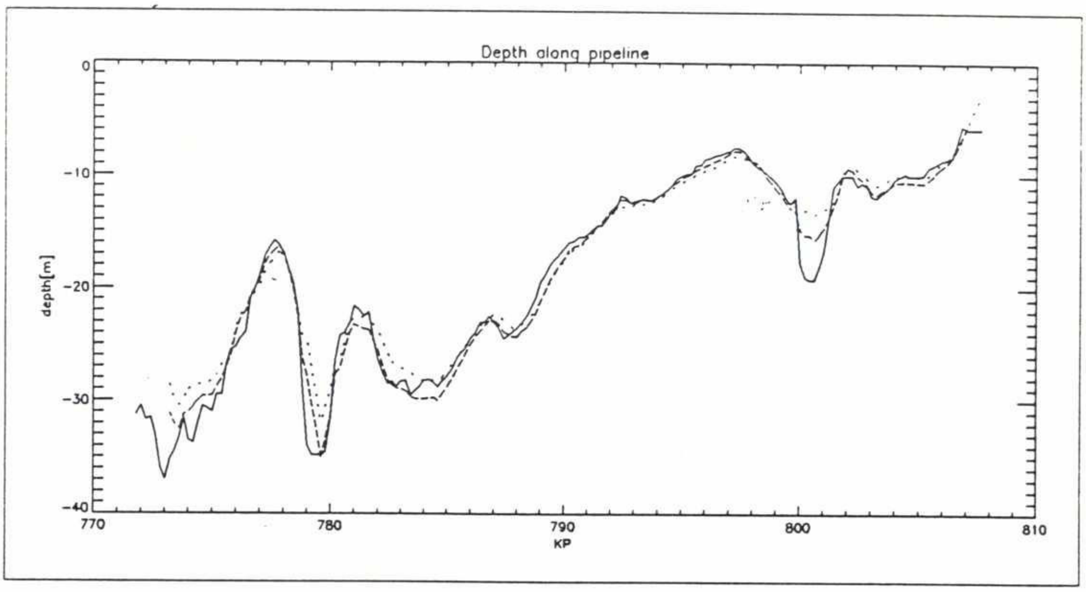

Figure 9 Comparison of sounding data (solid), pre-reconnaissance depth map (dashed) and Admiralty Chart data (dots)

Route Survey

The central track of the sounded area was digitized to reconstruct the reconnaissance survey (see solid line in Figure 3). Reconstructed data along this track were used to update the pre-reconnaissance depth map by extrapolation. The new data influenced the pre-reconnaissance depth map within a strip around the track. The width of this strip was determined by weight coefficients of the bathymetry model and was selected to be approximately 3 km; the result is shown in Figure 10. As the multibeam sounding data along the pipeline track were used for calibration, the pre-route depth map at the track equalled the measured depth. Depth errors along the track as observed in the pre-reconnaissance depth map were no longer present. The offtrack depth accuracy was assessed by comparing the pre-route depth map at a 100 m from the central track with depth measurements. The latter were reconstructed by digitizing the border of the sounded area. The results were bias 0 cm, rms 39 cm and abs 28 cm.

The pre-route depth map showed many details. As an example, at approximate coordinates 502,000 E and 5,712,000 N, the pipeline passed through a deep trough between two sand waves. A detailed contour plot of this site is given in Figure 11.

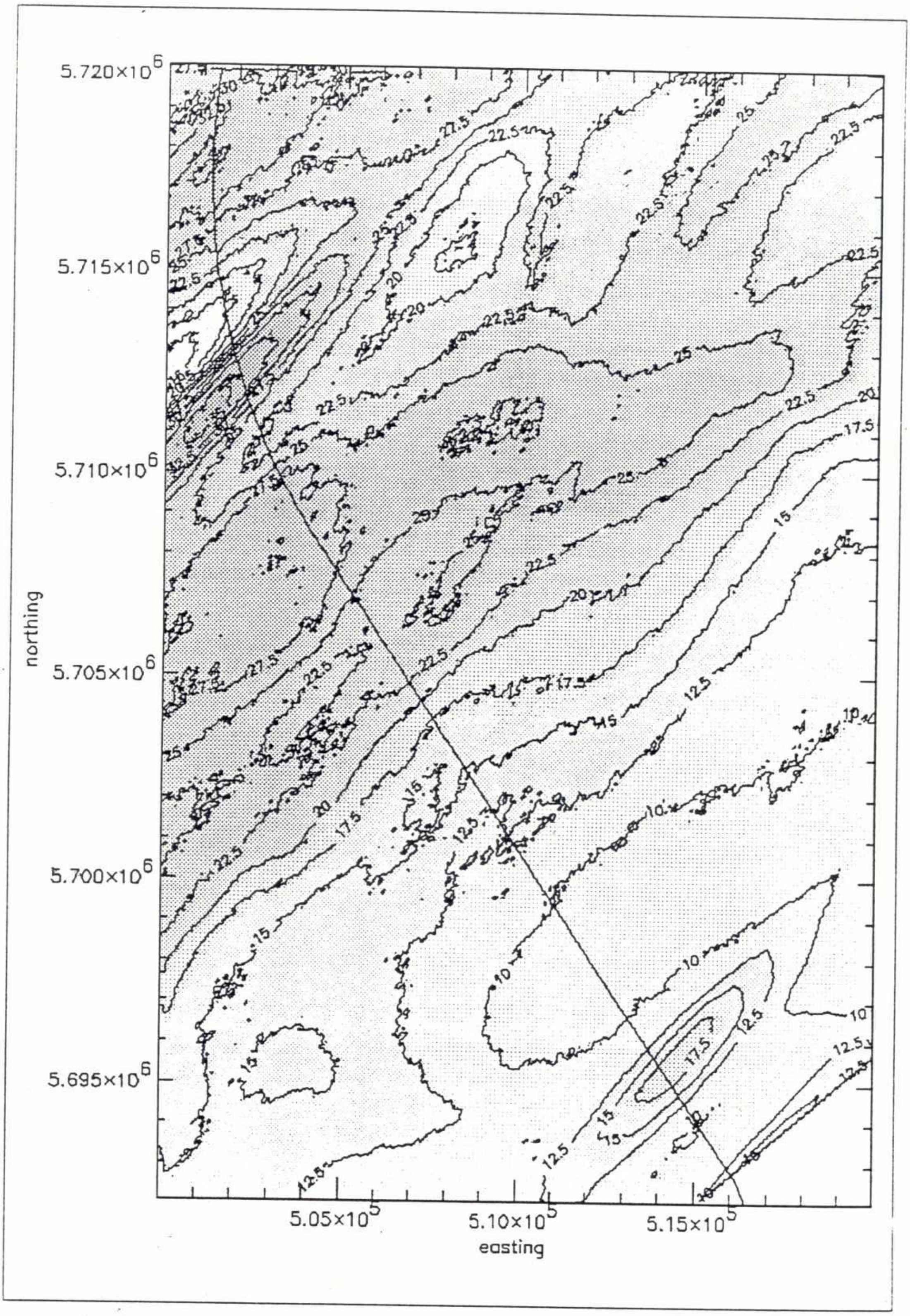

Figure 10 Pre-route depth map of bottom topography. Coordinates defined within UTM system. Line segment indicates track of pipeline

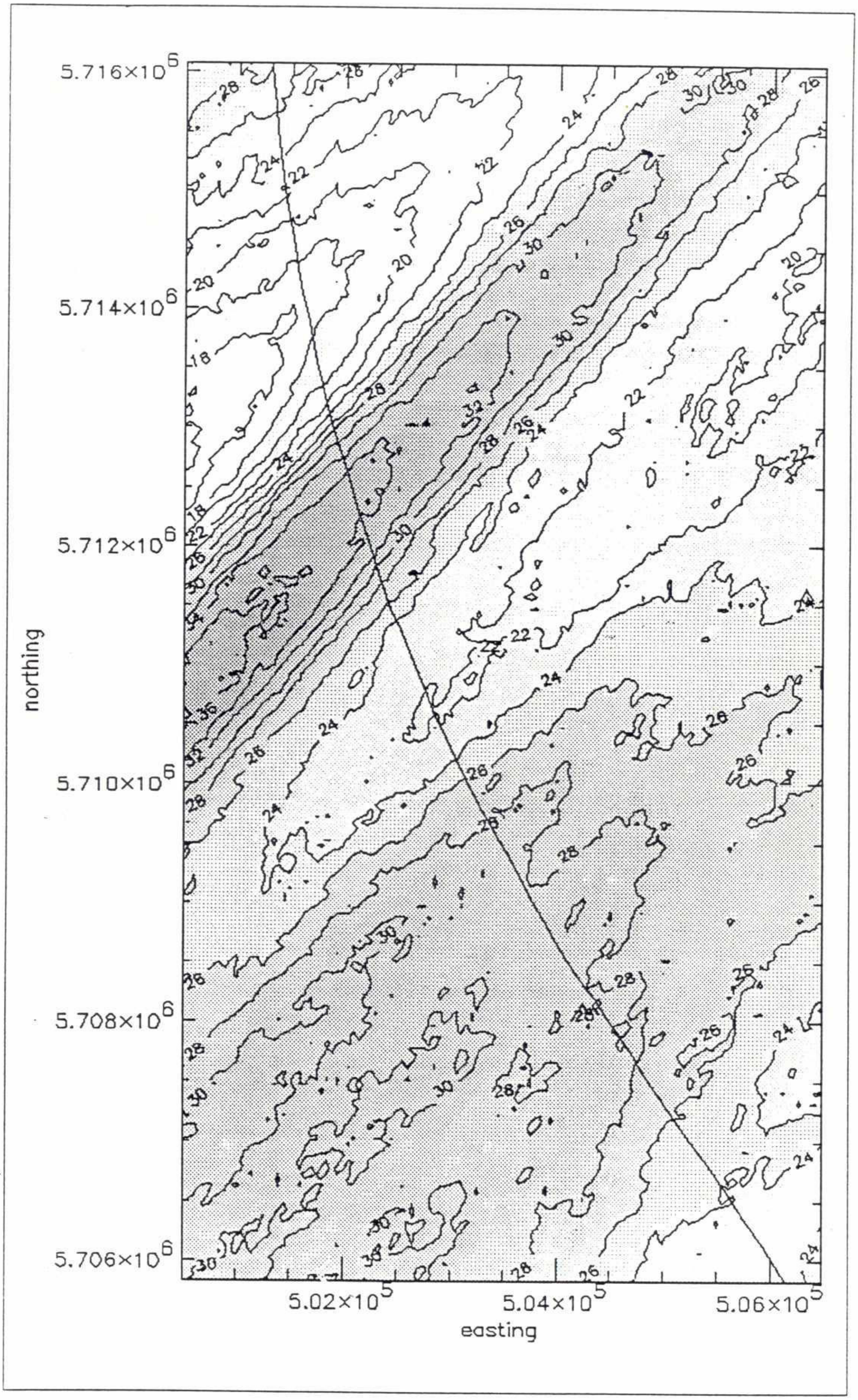

Figure 11 Detailed depth contours of part of the pre-route depth map. Contours are drawn at 2 m intervals

Pre-lay Survey

The central track and the two borders of the sounded area were digitized to reconstruct the route survey. The two outer tracks were then used to estimate the depth along the central track and the prediction errors using the Bathymetry Assessment System were found to be bias 0 cm, rms 26 cm and abs 18 cm. The soundings and the depth predictions were compared as shown in Figure 12. Depth along the central track was also estimated using linear interpolation. The prediction errors of this method were bias -1 cm, rms 32 cm and abs 21 cm. Both methods showed no significant bias. Results of both SAR-based and linear interpolation were compared with measurements in Figure 13. The Bathymetry Assessment System was slightly more accurate than the results of linear interpolation, especially in the channels. As expected, depth estimates based on linear interpolation underestimated the size of the depth modulations in these channels.

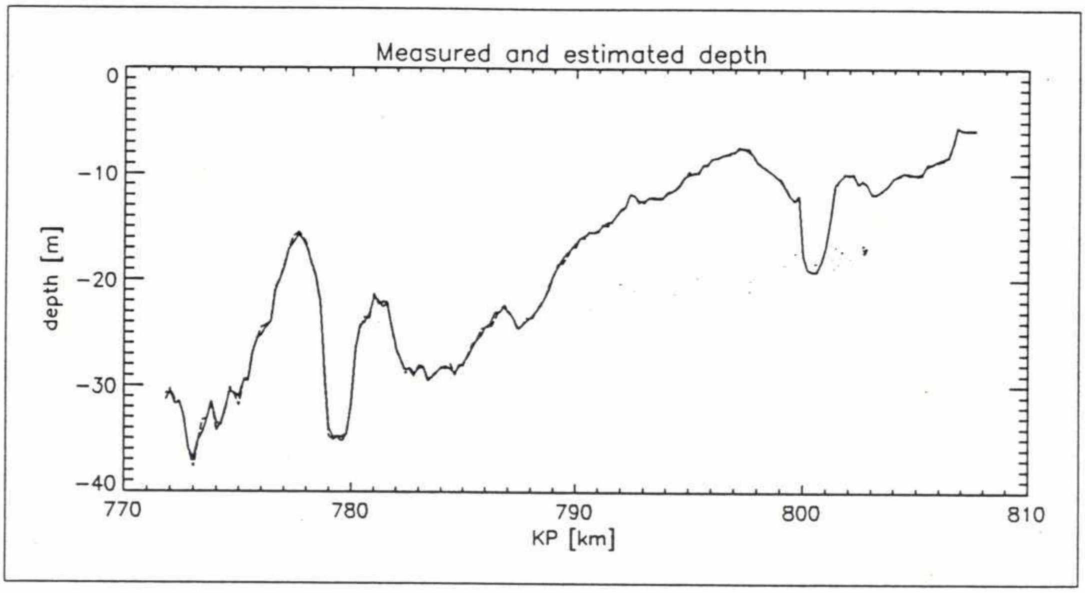

Figure 12 Depth estimates along the pipeline track. Solid: sounding data; dashed: estimated depth based on SAR data; dotted: estimated depth based on linear interpolation

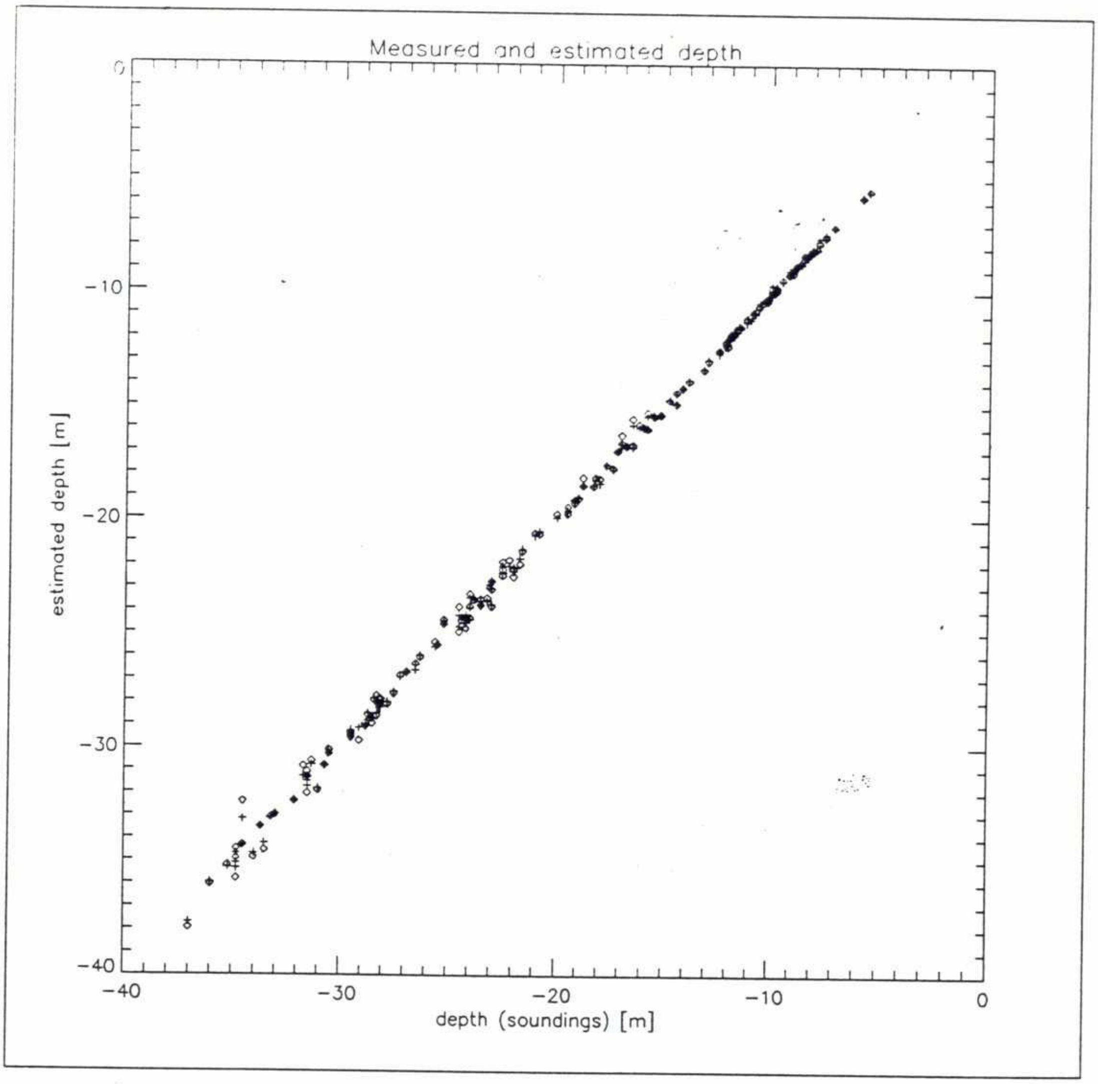

Figure 13 Scatter plot of measured and estimated depth along the pipeline track + depth based on SAR data; ◇ depth based on linear interpolation

7 Discussion

The maps generated for the three survey phases are discussed in this section .

Reconnaissance survey

The largest differences between pre-reconnaissance depth map and the sounding data were found along the track of the pipeline close to Zeebrugge (near KP 800, Figure 9). This was most probably due to the use of outdated calibration data and the hydro-meteorological conditions in this area.

(1) The pre-reconnaissance depth map was based on information from two data sources, namely, the Admiralty Chart and SAR imagery. The Admiralty Chart provided large-scale depth information, whereas the SAR imagery yielded the small-scale depth modulations. However, for medium-scale depth modulations a compromise between the sometimes conflicting information in both data sets had to be made. Since the depth in the channels as given by the Admiralty Chart was too low, the pre-reconnaissance depth map tended to yield depth values that were also correspondingly low.

(2) According to the "Admiralty Tide Tables" and "Tidal Stream Tables", the flow velocity in the area close to Zeebrugge was less than 0.1 m/s at the time of image recording which is rather low. In addition, the tidal stream atlas of the North Sea indicated that the tidal current was directed towards the shore and split in two separate flows just before Zeebrugge harbour. This resulted in a low signal to noise ratio and so depth estimates in this area as obtained by means of the bathymetry model were less reliable than those in areas further offshore.

Route survey

Survey data from the reconnaissance survey were extrapolated perpendicular to the surveyed track. The quality of this extrapolation was determined at a distance a 100 m from the track. Depth was estimated with an accuracy of 40 cm but no information about the position of ship wreckage and other uncharted obstacles could be provided.

Pre-lay survey

The interpolation accuracy was assessed for a distance of 200 m between section lines. With the given data it was not possible to reconstruct route survey data at larger offsets to the track. However, an indication of the potential of SAR data for interpolation between section lines further apart was given by simulating an across-track survey.

An across-track route survey was reconstructed by digitizing section lines perpendicular to the pipeline track. For several pairs of section lines the depth in between was estimated using the bathymetry model and linear interpolation. The results are given in Table 3.

Distance between section lines [m]	Bias [cm]		rms [cm]		abs [cm]	
	SAR	linear	SAR	linear	SAR	linear
2 x 100	0	0	34	40	24	25
2 x 200	0	0	52	60	36	37
2 x 400	0	0	77	119	56	75
2 x 600	0	0	91	176	68	116
2 x 800	0	-1	99	245	77	153
2 x 1000	0	-1	102	320	77	200

Table 3 Comparison of depth estimation errors of the bathymetry model (first number in each column) and linear interpolation (second number in each column) as a function of the distance between the section lines. "Bias" indicates the average difference between soundings and estimate, " rms" indicates the root mean square difference, "abs" the average absolute difference and "max" the maximum absolute difference

Both the SAR based method and linear interpolation showed no significant bias and at short distances both methods yielded similar results, as could be expected. "Rms" and "abs" errors increased with distance but the rms errors of the bathymetry model tended to saturate to a maximum whereas the rms error of the linear interpolation method increased continuously. At an offset of more than a 1000 m, the estimated depth based on linear interpolation became unrelated to the actual depth.

The accuracies obtained in this report are minimum results and it is expected that in the future these results will be improved due to the following factors:

- The models of the bathymetry system will be improved so that they better can be applied in complex, two-dimensional situations. In Section 6 it was already noted that close to Zeebrugge harbour a two-dimensional current pattern was observed.
- The optimization routines in the bathymetry system will be improved, resulting in smoother depth assessments.
- The SAR images used in this report were selected based on tidal information. However, the images were also contaminated with speckle noise which adversely affected the quality of the depth assessment. It is expected that under better hydro-meteorological conditions SAR images can be acquired which are better suited for the assessment of the bottom topography along the ZEEPIPE strip.
- L-band SAR systems, as mounted on the Japanese satellite JERS-1, are better suited for mapping the bottom topography of shallow seas than a C-band system as used by the ERS-1. Presently, the quality of ERS-1 sea-mode SAR imagery is superior, but high quality L-band systems are expected to be launched in the coming decade.

Cost comparison

As an example we will present in the following a cost comparison for an area of 10 x 30 km^2. Depth estimates are obtained with a spatial resolution of 30 m for both the SAR-based method whereas the tracks surveyed by the traditional method are assumed to are assumed to ly at distances of 200 m.

A. Cost of SAR imagery acquisition, processing and reporting, excluding field control surveys, approximate cost US$ 60,000.

B. Cost estimate for traditional echosounding over the same area and surveyed at 200 m interval.

Total survey line	:	1500 km
Average survey speed (fast)	:	6 knots
Approximate total survey days	:	135 days
Average survey cost per day	:	US$ 5,000

Approximate total project estimate is US$ 675,000, excluding weather allowances, breakdowns and all other events.

The figures presented are indicative, actual costs of a traditional survey depend on the type of ship being used, size of the crew, etc.

This cost estimate can be made for each phase of the pipeline project, assuming a track length of 30 km. Results are presented in Table 4. Table 4 also shows the accuracy of the results obtained using traditional methods and the BAS.

Traditional			**Bathymetry Assessment System**			
information	rms accuracy	costs US$	information	method	rms accuracy	costs US$
Admiralty Chart	214 cm whole area	40	Admiralty Chart + ERS-1 data	inverse modelling	135 cm whole area	30,000
Reconnaisance survey: 1 track						
+ single track	20 cm along track, 214 cm elsewhere	15,000	+ single track	extrapolation using ERS-1	20 cm along track 39 cm in 200 m corridor	15,000
Route survey: 2 additional tracks						
+ 2 border scans	20 cm along tracks	30,000	+ 2 border scans	interpolation using ERS-1	26 cm in 200 m corridor	15,000
Pre-lay survey: 15 scans in 200 m corridor						
15 scans in 200 m corridor	20 cm in 200 m corridor	203,000				
	Total	248,000			Total	60,000

Table 4 Comparison of data provided by traditional methods and the Bathymetry Assessment System

8 Conclusions

To plan the consecutive stages, namely, reconnaissance, route and pre-lay survey, three maps have been made. These maps are based on existing data (such as Admiralty Charts), SAR imagery and sounding data acquired in the previous phase of the pipeline project. The accuracies of the maps are compiled in Table 5.

	bias [cm]	rms [cm]	abs [cm]
Admiralty Chart data	75	214	127
Pre-reconnaissance depth map	49	135	90
Pre-route depth map	0	39	28
Pre-lay depth map	0	26	18

Table 5 Comparison of depth maps and sounding data. Admiralty Chart data and pre-reconnaissance depth map are compared with sounding data at the pipeline track. Accuracy of the pre-route depth map is assessed at a 100 m from the track and the pre-lay depth map is based on section lines that lie at a distance of 200 m

It is concluded that:

- It is possible to construct up-to-date large-scale depth maps based on remote sensing data and existing Admiralty Chart data. For example, it was found that the maximum error in the pre-reconnaissance depth map was 4.78 m less than the maximum error in the Admiralty Chart. Based on such a map the reconnaissance survey can be optimized.

- Using the data from reconnaissance survey an improved pre-route depth map can be constructed by extrapolation. This may result in the generation of better alternatives for the route survey.

- Using the data from the route survey the depth map can be improved further by interpolation between section lines.

- Interpolation using SAR data yields better results than those achievable by linear interpolation.

- Absolute accuracy achieved by combination of ERS-1 SAR and echosounding was of the order of 30 cm which is comparable to most industry-standard echosounders.

Therefore, it appears technically feasible to optimize survey effort using ERS-1 SAR imagery. In general the effect of ERS-1 SAR imagery on the accuracy of the depth assessment and the potential reduction in survey effort depends on the actual *in-situ* topography. The actual cost savings through the reduction of ship's soundings depend on the user requirements with respect to the desired depth accuracy and survey area.

9 Acknowledgements

Thanks are due to ESA for the prompt delivery of the analyzed SAR imagery. Further we thank NORSKE STATS OLJESELSKAP (STATOIL) for their kind permission to use the ZEEPIPE survey data.

References

Alpers, W., and Hennings, I., A Theory of the Imaging of Underwater Bottom. Topography by Real and Synthetic Aperture Radar, *Journal of Geophysical Research*, Vol. 89, No. C6, pp 10,529-10,546, November 20, 1984.

Calkoen, C.J., Kooi, M.W.A. van der, Hesselmans, G.H.F.M., and Wensink, G.J., *The imaging of sea bottom topography with polarimetric P-, L-, and C-band SAR.* Report BCRS project 2.1/AO-02. Netherlands Remote Sensing Board. Delft 1993.

Vogelzang, J., Wensink, G.J., de Loor, G.P., Peters, H.C. Pouwels, H., and van Gein, W.A., 1989, *Sea bottom topography with X-band SLAR*, BCRS report, BCRS-89-25.

• location 'De Voorst'

• main office

main office
Rotterdamseweg 185
p.o. box 177
2600 MH Delft
The Netherlands
telephone (31) 15 - 56 93 53
telefax (31) 15 - 61 96 74
telex 38176 hydel-nl

location ' De Voorst'
Voorsterweg 28, Marknesse
p.o. box 152
8300 AD Emmeloord
The Netherlands
telephone (31) 5274 - 29 22
telefax (31) 5274 - 35 73
telex 42290 hylvo-nl

North Sea

• Amsterdam

• London

Brussels •

W2

Appendix D

River bathymetry observation with radar remote sensing

Reprint of paper "River bathymetry observation with radar remote sensing"
by
E.Mosselman and G.J.Wensink,
presented at the International Workshop on the Morphological Behaviour of the Major Rivers in Bangladesh, held in Dhaka in November 1993.

26

The International Workshop on Morphological Behaviour of Major Rivers in Bangladesh
The Dhaka Sheraton Hotel, Dhaka, Bangladesh, 6-8 November 1993

RIVER BATHYMETRY OBSERVATION WITH RADAR REMOTE SENSING

by

E. Mosselman[1,2] and G.J. Wensink[2]

ABSTRACT

Remote sensing has proven to be a valuable tool for the study and the prediction of morphological changes in the Brahmaputra-Jamuna River. The traditional optical and infrared bands of the electromagnetic spectrum, however, do not penetrate clouds or turbid water. This restricts their use in Bangladesh to the dry season, whereas the most significant morphological changes occur during the monsoon. Radar remote sensing does not have this restriction. It penetrates clouds directly and allows the observation of bathymetry under clear or turbid water in an indirect way. We explain the underlying mechanisms and present our experiences with radar observation of sand waves in a 22 meter deep area of the North Sea. Based on that, we discuss the possible application to the Brahmaputra-Jamuna River.

1 HISTORICAL BACKGROUND

It is known for some time now that under suitable conditions (moderate wind and strong tidal current) the sea bottom topography is visible in images taken by Side Looking Airborne Radar (SLAR) and Synthetic Aperture Radar (SAR). De Loor discovered this phenomenon in 1969 in Q-band SLAR imagery of the North Sea (de Loor & Brunsveld van Hutten, 1978; de Loor, 1981). These images were made off the Dutch coast to study the detection of waves and swell directions. The images revealed some kind of wave patterns which were originally believed to be caused by swell. However, the patterns had a fixed position and disappeared during high and low tide when the tidal flow velocity vanished. Then it was realized that these patterns were caused by sand waves on the bottom of the sea. At first this phenomenon was considered a disturbing factor, obscuring oil spills in radar images, and little attention was paid to it. This changed drastically after the SEASAT mission in 1978. SEASAT carried an L-band SAR that recorded spectacular images of bottom topography in shallow seas like the Southern Bight of the North Sea (Alpers & Hennings, 1984), the English Channel (Lodge, 1983) and the Nantucket Shoals (Shuchman & al, 1985). The SEASAT mission demonstrated the potential of radar remote sensing and stimulated much further experimental and

---

[1] Consulting Consortium FAP 21/22.

[2] DELFT HYDRAULICS, P.O. Box 152, 8300 AD Emmeloord, The Netherlands.

theoretical research (e.g. Vogelzang & al, 1992).

In the year of de Loor's bench-mark discovery of sea bed topography in radar images, Coleman's (1969) bench-mark paper on the Brahmaputra River appeared. The Brahmaputra-Jamuna River is characterized by extremely rapid morphological changes, mainly occurring during the monsoon. Remote sensing has been used since the late 1960s for the study of those changes and their underlying mechanisms, initially from aircraft (Coleman, 1969) but later also from satellites (Bristow, 1987; Klaassen & Masselink, 1992; Klaassen & al, 1993; Sir William Halcrow & Partners, 1993; ISPAN, 1993; Hartmann & al, 1993; Mosselman & al, 1993). Many people agree that radar remote sensing would be even better than the optical and infrared remote sensing used till now, because radar penetrates the clouds that are ubiquitous during the monsoon. The penetration of clouds, however, is not the only advantage. There is also the possibility that the *bathymetry* of the Brahmaputra-Jamuna River can be observed with radar in a similar way as the bottom topography of shallow seas in Europe and America.

2 THEORY

At first glance it might seem strange that bathymetry can be observed by radar while radar radiation is fully reflected by the water surface. The observation, however, is not direct but indirect, see Figure 1. Variations in bed level produce modulations in surface flow velocities. The latter cause variations in the spectrum of water surface waves and hence variations in water surface roughness. Radar backscatter is a function of surface roughness. When radar radiation strikes the surface under an angle, a perfectly smooth surface would act as a mirror, reflecting all radiation away from the radar. The rougher the surface is, the more power is backscattered into the radar and the brighter the surface appears in the image. The Maxwell equations provide the general description for this mechanism, but they can be simplified for particular cases. The most relevant simplification here is valid for incidence angles between 20° and 70°. The backscatter can then be described as first-order *Bragg scattering*. This is resonant scattering which occurs when the water waves have the same wave length as the incident radiation, corrected for the angle of incidence. The water waves that produce this Bragg scattering are called *Bragg waves*. Their wave length is on the order of centimeters. The wave spectrum variations that carry the information on bathymetry and that are detected by radar, are in fact modulations in the Bragg waves.

The imaging mechanism described above implies that radar images can also be constructed through computation in the following three steps:

(1) Computation of the modulations in surface flow velocities due to interaction between flow and bed topography. Such computations are generally based on equations describing the conservation of both mass and momentum of elementary volumes of water, but sometimes the equation for the conservation of mass, or continuity equation, is sufficient.

(2) Computation of the variations in the wave spectrum due to modulations in surface flow velocities. This computation is based on the action balance equation (Hasselmann, 1960; Willebrand, 1975).

(3) Computation of the modulations in radar backscatter due to variations in the wave spectrum. These modulations are modelled with first-order Bragg scattering or with two-scale models in which Bragg scattering and Kirchhoff scattering (specular reflection) are combined.

These steps form the basis of a data assimilation technique for quantitative bathymetry assessment. The procedure starts with an assumed bed topography. Numerical models for (1) water flow, (2) generation and advection of waves and (3) radar backscattering are used to compute a corresponding radar image. Evaluation of the differences between this simulated radar image and the real radar image reveals the required adjustments of the assumed bed topography. A new radar image is computed in the same way from the adjusted bed topography and this whole procedure is repeated until the differences between the simulated and the real image are smaller than a prescribed accuracy level. The bed topography thus obtained is approximately equal to the real bathymetry.

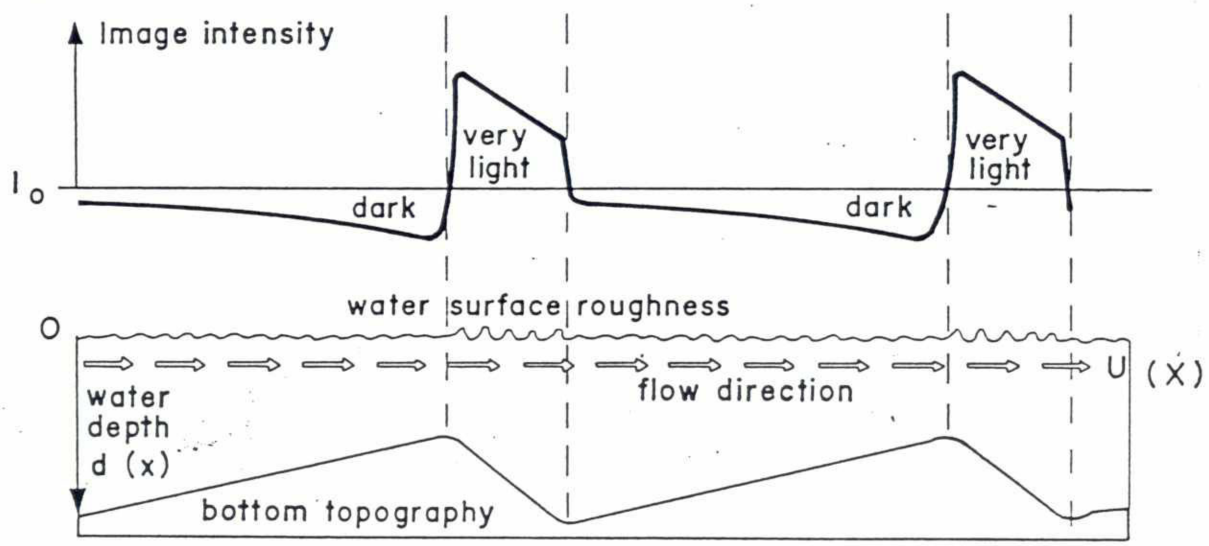

Fig. 1 Imaging mechanism.

3 EXPERIMENT IN THE NORTH SEA

An experiment was carried out in the North Sea off the Dutch coast on August 16, 1989. The main sensor was the NASA/JPL Airborne Imaging Radar (AIR), which is a three-band (P-, L- and C-band) multi-polarization SAR carried aboard a modified DC-8 passenger jet. The recorded area is shown in Figure 2. The hydro-meteo conditions during the experiment were excellent for observing bottom topography. Though a wind speed of at least 10 m/s was predicted on the day before, it reduced to around 5 m/s from the Southwest during the experiment. Flow velocities and directions were measured from a ship of Rijkswaterstaat, the Octans. The surface flow velocity was around 0.6 m/s, directed towards the Southwest, i.e. opposite to the wind.

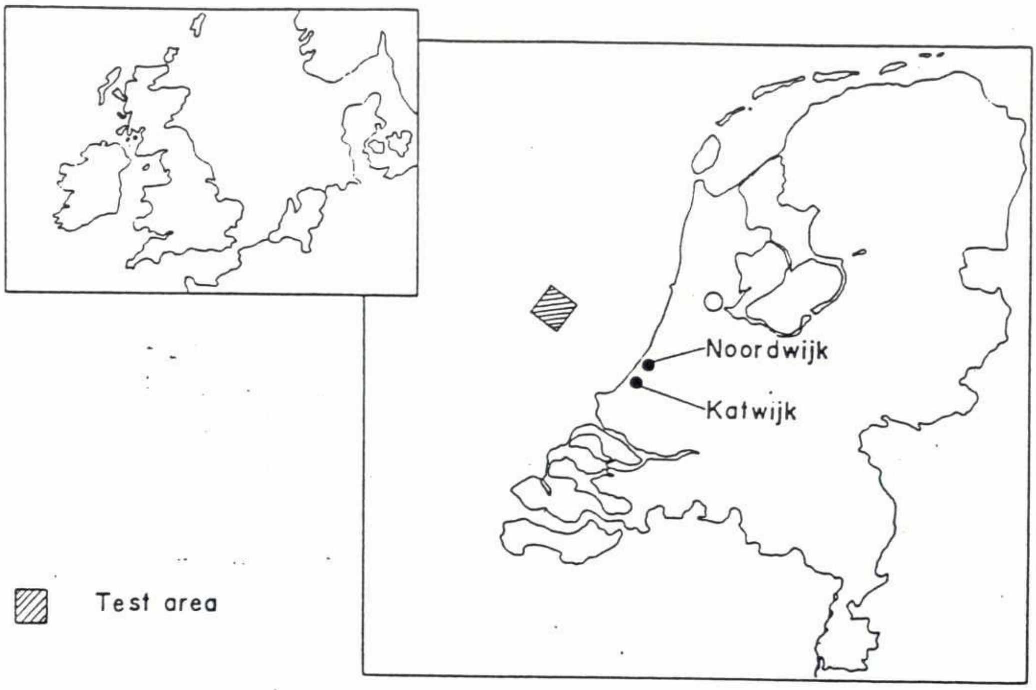

Fig. 2 Test area in the North Sea.

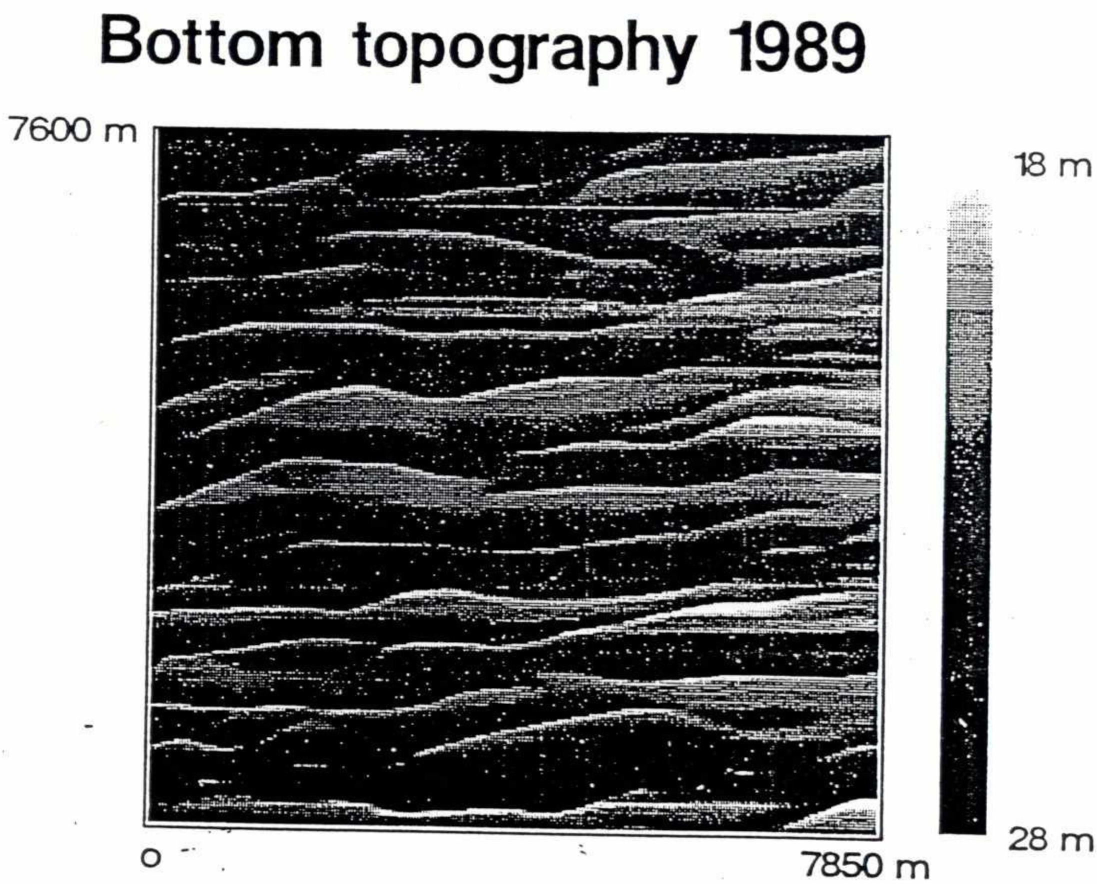

Fig. 3 North Sea bathymetry derived from radar observation.

The results are shown in Figure 3. The bottom topography is dominated by sand waves with a height between 2 m and 6 m and an average crest-to-crest distance of 400 m at an average water depth of about 22 m. The sand waves have an asymmetrical profile, more like a saw-tooth than a sine. The best results were obtained in the P-band, poor results in the L-band and no results in the C-band. Observations in the C-band are disturbed by floating layers and wind field inhomogeneities. The results are not (yet ?) as precise as the results from traditional bathymetric surveys, but radar imagery gives an overview of large areas in a quick and cheap way and can therefore be used to optimize bathymetric surveys.

4 POSSIBLE APPLICATION TO THE BRAHMAPUTRA-JAMUNA RIVER

Bathymetry patterns in the Jamuna River are visible in an ERS-1 radar image of July 24, 1993. The bathymetry is still to be assessed quantitatively with numerical models.

The feasibility of the technique for the Brahmaputra-Jamuna River depends also on the statistical distributions of the hydro-meteo conditions. The most favourable conditions for radar bathymetry observation in the North Sea are found to be a strong flow velocity of more than 0.4 m/s and a moderate wind speed between 4 and 10 m/s (3 - 5 Bft). The minimum wind speed at which backscatter from the water surface is detectable, depends on the sensitivity of the radar system. Flow velocities in the Brahmaputra-Jamuna River are high enough, but wind speeds might often be too low to generate detectable waves. On the other hand, waves due to high Froude number flow might also produce variations in water surface roughness which can be detected by radar. We observed these waves during site visits by boat on September 17 and 18, 1993, and the local Executive Engineer of BWDB confirmed that the areas with these waves corresponded to the locations of the deep channels (Hoque, 1993).

The flow in the Brahmaputra-Jamuna River is more complicated than the rather uniform tidal flow in the North Sea. This means that the continuity equation will not be sufficient for computing the modulations in surface flow velocities. The momentum equation will have to be used as well.

It is interesting to note that optical backscatter of solar radiation (sun glint) can locally produce similar results as radar backscatter. This is for instance visible in aerial photographs of the Brahmaputra-Jamuna River from 1990. Overlap areas are present on pairs of successive photographs taken only a few seconds apart. The area is often bright on one photograph due to sun glint, but of normal intensity on the other photograph because of the different angle of incidence. The bright reflection from the water surface sometimes displays submerged bed patterns that are not visible on its neutral counterpart. Nevertheless, assessing bathymetry from this optical backscatter is not a feasible technique.

Synoptic bathymetric observations during the monsoon would serve many purposes. First of all they would allow a more detailed study of the morphological processes by increasing the temporal resolution of the remotely sensed data. Secondly, by making frequent updates of the morphological developments possible, they would improve the predictions of bank erosion at sites for bank protection and river training works (FAP 21). And last but not least, they could play a central role in active flood plain management (FAP 22) where they could be used for the selection of locations and for the monitoring of the efficiency of recurrent measures.

২৮

5 CONCLUSION AND RECOMMENDATION

River bathymetry observation with radar is a promising technique. We recommend to start with a pilot project in which the bathymetry of a part of the Brahmaputra-Jamuna River is inferred from radar imagery and verified against other sources of information.

REFERENCES

Alpers, W. & I. Hennings (1984), A theory of the imaging mechanism of underwater bottom topography by real and synthetic aperture radar. J. Geophys. Res., 89 C, pp.10529-10546.

Bristow, C.S. (1987), Brahmaputra River: channel migration and deposition. In: Recent developments in fluvial sedimentology, Soc. Economic Paleontologists and Mineralogists, Spec. Publ. 39.

Coleman, J.M. (1969), Brahmaputra River: channel processes and sedimentation. Sedimentary Geol., 3, 2-3, pp.129-239.

Hartmann, R.A., J. Rupke & A.C. Seymonsbergen (1993), The influence of neo-tectonic movements on the planform development of the Jamuna river, Bangladesh. A preliminary appraisal on the basis of Landsat MSS images. Alpine Geomorphology Research Group, Univ. of Amsterdam (limited distribution).

Hasselmann, K. (1960), Grundgleichungen der Seegangsvorhersage. Shiffstechnik, 7, pp.191-195 (in German).

Hoque, M.A. (1993), Personal communication. Bangladesh Water Development Board, Gaibandha O&M Division.

ISPAN (1993), The dynamic physical and socioeconomic environment of riverain charlands: Brahmaputra-Jamuna. Environmental Study (FAP 16) and Geographic Information System (FAP 19), Rep. to FPCO.

Klaassen, G.J. & G. Masselink (1992), Planform changes of a braided river with fine sand as bed and bank material. Proc. Fifth Int. Symp. River Sedimentation, Karlsruhe, pp.459-471.

Klaassen, G.J., E. Mosselman & H. Brühl (1993), On the prediction of planform changes in braided sand-bed rivers. Adv. in Hydro-Sci. and -Engrg., Ed. S.S.Y. Wang, pp.134-146.

Lodge, D.W.S. (1983), Surface expression of bathymetry on SEASAT synthetic aperture radar images. Int. J. Remote Sensing, 4, pp.639-653.

Loor, G.P. de & H.W. Brunsveld van Hulten (1978), Microwave measurements over the North Sea. Boundary Layer Meteorology, 13, pp.113-131.

Loor, G.P. de (1981), The observation of tidal patterns, currents and bathymetry with SLAR imagery of the sea. IEEE J. Oceanic Engrg., OE-6, pp.124-129.

Mosselman, E., M. Huisink, E. Koomen & A.C. Seymonsbergen (1993), Morphological changes in a large braided sand-bed river. Third Int. Geomorphol. Conf., Hamilton, Ontario.

Shuchman, R.A., D.R. Lyzenga & G.A. Meadows (1985), Synthetic Aperture Radar imaging of ocean-bottom topography via tidal-current interactions: theory and observations. Int. J. Remote Sensing, 6, pp.1179-1200.

Sir William Halcrow & Partners (1993), River training studies of the Brahmaputra River; Annex 2: Morphology. Rep. to BWDB.

Vogelzang, J., G.J. Wensink, G.P. de Loor, H.C. Peters & H. Pouwels (1992), Sea bottom topography with X-band SLAR: the relation between radar imagery and bathymetry. Int. J. Remote Sensing, 13, pp.1943-1958.

Willebrand, J. (1975), Energy transport in a nonlinear and inhomogeneous random gravity wave field. J. Fluid Mech., 70, pp.113-126.